Relative radiometric correction methods for remote sensing images and their applicability analysis

DUAN Yini[1,2], ZHANG Lifu[2], YAN Lei[1], WU Taixia[2], LIU Yuesheng[3], TONG Qingxi[1,2]

1. *RS&GIS Institute*, *Peking University*, *Beijing* 100871, *China*;
2. *Institute of Remote Sensing and Digital Earth*, *Chinese Academy of Sciences*, *Beijing* 100101, *China*;
3. *Beijing Institute of Information Technology*, *Beijing* 100035, *China*

Abstract: Relative radiometric correction of remote sensing images is a basic data preprocessing technique used to eliminate r adiometric problems in images such as non-uniformity, stripe noises, and defective lines. Over the past 30 years, numerous relative radiometric correction methods and algorithms have been developed. This situation brings up three questions. (1) What are the differences and relationships among these methods? (2) What are the characteristics of each method? (3) How is a suitable method selected? To answer these questions, the methods are first classified into three categories: calibration-based, scene-based, and c omprehensive methods. Second, the mathematical models of the three categories of methods are provided in the new classification system. Then, each method is introduced and compared with the others. Third, the applicability of the methods is comprehensively analyzed according to the following aspects: non-uniformity characteristics, geometric characteristics, sensor calibration, and the comprehensive characteristics of images. Suggestions on selecting a suitable method are provided, and an example of image correction is demonstrated. Finally, the research tendency and several existing problems of relative radiometric correction are analyzed. The computer criteria for signal and noises, the evaluation system, and the influence on subsequent absolute corrections require f urther studies.

Key words: relative radiometric correction, calibration-based relative radiometric correction method, scene-based relative radiometric correction method, comprehensive relative radiometric correction method, applicability analysis

CLC number: P23/TP751 **Document code**: A

Citation format: **Duan Y N, Zhang L F, Yan L, Wu T X, Liu Y S and Tong Q X. 2014. Relative radiometric correction methods for remote sensing images and their applicability analysis. Journal of R emote Sensing, 1 8(3): 597 - 617 [DOI: 10. 11834/jrs. 20143204]**

1 INTRODUCTION

Relative radiometric correction is sometimes called destriping or non-uniformity correction. This process involves correcting an original remote sensing image by using relative r adiometric correction coefficients to eliminate radiometric non-uniformity caused by different responses of remote sensors or Charge-Coupled Device (CCD) detectors (Dinguirard & Slater, 1999). According to the gradation rule for remote sensing satellite data products, relative radiometric correction is the level 1 product of radiometric calibration, which occurs prior to absolute radiometric calibration, atmospheric correction, and topographic radiometric correction. Therefore, relative radiometric correction is the basis for radiometric correction (Wang, et al., 2013; Du & Zhao, 2006).

Non-uniformity problems of remote sensing images include three main types: radiometric non-uniformity within the entire image, stripe noises, and defective lines. For many spaceborne and airborne remote sensors, the occurrence of various radiometric problems in their images during long-term operation is common. These problems are typically caused by different r esponses of optical systems (e. g., different optical transmittance for different parts of alens), different responses of CCD detectors, broken detectors, dark currents in CCDs, different e lectronic links outside CCDs, and so on; such problems can be solved by relative radiometric correction (Corsini, et al., 2000; Chander, et al., 2002; Henderson & Krause, 2004).

Research on relative radiometric correction has a history of more than 30 years. Singh (1985) developed a calibration-based relative radiometric correction method that uses the internal calibration system of Landsat. Consequently, radiometric correction coefficients were acquired through this method. The scene-based relative radiometric correction method, which is a substitute for correcting Landsat images, was used to validate the correction precision of scene-based methods. Scene-based methods have not

Received: 2013-07-23; **Accepted**: 2013-10-28; **Version of record first published**: 2013-11-05

Foundation: National High Technology Research and Development Program of China (863 program) (No. 2012AA121504-2); Special Research Funding for Public Benefit Industries from the National Ministry of Environmental Protection (No. 2011467071)

First author biography: DUAN Yini (1988—), female, Ph. D. candidate, her majors are remote sensor calibration and radiometric correction. E-mail: yiniduan@126. com

Corresponding author biography: ZHANG Lifu (1967—), male, professor. His research interests are hyperspectral remote sensing and its applications. E -mail: zhanglf@ irsa. ac. cn

been widely used (Horn & Woodham, 1979) until the internal calibration of Landsat was invalidated. Recently, in addition to these methods, numerous relative radiometric correction methods and algorithms have been developed (Gao, et al., 2011; Gladkova, et al., 2012). This situation brings up three questions. (1) What are the differences and relationships among relative radiometric correction methods? (2) What are the characteristic of each method? (3) How is a suitable method selected?

To answer these questions, previous relative radiometric correction methods are first summarized. Then, the basic ideas and principles, as well as the advantages and disadvantages of each method, are presented and compared in detail. Finally, the applicability of different methods is comprehensively discussed, and suggestions are provided on selecting a suitable method.

2 CLASSIFYING RELATIVE RADIOMETRIC CORRECTION METHODS

At present, two classification rules are employed for relative radiometric correction methods. One rule classifies methods by acquiring correction coefficients. Ratliff, et al. (2003) and Guo, et al. (2005) divided relative radiometric correction methods into two categories: calibration-and scene-based relative radiometric correction methods. Calibration-based relative radiometric correction methods include laboratory and internal calibration-based methods. Scene-based relative radiometric correction methods include homogeneous scenes, histogram equalization, and histogram matching. The other rule classifies methods based on the principles of algorithms. Chen, et al. (2003) divided destriping algorithms into four categories: histogram matching, moment matching, digital filtering, and radiometric equalization. diBisceglie, et al. (2009) divided destriping methods and algorithms into three categories: statistical matching method, spatial filtering, and radiometric equalization. Jung, et al. (2010) categorized the destriping approach by filtering techniques and by adjusting the distribution of brightness values for each detector to ascertain reference distribution.

With the recent rapid increase in various remote sensing data, a series of new developments has been reported in the field of relative radiometric correction. New characteristics emerge in relative radiometric correction methods and algorithms, which can be summarized into three aspects. First, the application fields of calibration-based methods increase. In addition to internal calibration, other calibration approaches such as outdoor calibration and ground-based calibration can be used to obtain calibration coefficients for image correction. As a result, calibration-based methods can now be used in more cases during different phases of a remote sensor (Duan, et al., 2013; Bindschadler & Choi, 2003). Second, the algorithms of scene-based methods significantly increase. Based on traditional histogram equalization, histogram matching, and moment matching, several improved algorithms have been developed (Liu, et al., 2002; Pan, et al., 2005). To eliminate stripe noises, spatial filtering and frequency filtering techniques have been introduced from the field of digital image processing and have developed into numerous filtering algorithms for remote sensing images (Zhang, et al., 2006; Yang, et al., 2003). New mathematical models and interdiscipline have also resulted in the development of new algorithms such as the Maximum A Posteriori (MAP)-based algorithm for destriping and in painting remotely sensed images as well as an uneven illumination correction method based on variational retinex for remote sensing images (Shen & Zhang, 2009; Li, et al., 2010). To take advantage of the high correlation among different bands of a hyperspectral image, a subspace-based striping noise reduction algorithm and spectral moment matching were developed (Acito, et al., 2011; Sun, et al., 2008). Third, the trend is toward using different combinations of methods and algorithms such as relative radiometric correction methods based on laboratory calibration and homogeneous scenes, stripe noise reduction by combining histogram matching with a facet filter, and image restoration by combining stripe detection and spline functions (Zeng, et al., 2012; Rakwatin, et al., 2007; Fuan & Chen, 2008).

From these analyses, we learn that the classification rule proposed by Ratliff and Guo, et al. (2005) can clearly divide different relative radiometric correction methods and algorithms under a macroscopic perspective; however, comprehensive relative radiometric correction methods do not follow this classification rule. The classification rule proposed by Chen (1997), diBisceglie, et al. (2009), Jung, et al. (2010). focuses on classifying scene-based methods without considering calibration-based methods. To solve this problem, the current study proposed a new classification rule that fully considers the ideas and characteristics of previous classification rules. As shown in Fig. 1, the new classification rule divides all relative radiometric correction methods into three categories: calibration-based, scene-based, and comprehensive relative radiometric correction methods. Moreover, this classification rule divides each category into subcategories. Hence, this rule does not only present the differences and relationships among various methods and completely covers the previous methods but it also exhibits high scalability. The dashed lines in Fig. 1 show that comprehensive methods have the characteristics of both calibration- and scene-based methods, and include two cases: the combination of different algorithms of scene-based methods and the combination of the calibration-and scene-based methods.

2.1 Calibration-based methods

Calibration-based methods are used to acquire relative radiometric correction coefficients through sensor calibration. These coefficients are used to correct the original remote sensing image. Given that relative radiometric correction coefficients are derived from calibration experiments, calibration-based methods require special training data. The mathematical model of calibration-based methods is illustrated in Fig. 2, where $X(i)$ refers to the original remote sensing image, $C(i)$ refers to the training data, $S(i,C(i))$ is the calibration model, and $Y(i)$ is the corrected image. Thus, $Y(i)=X(i)S(i,C(i))$.

Based on different stages of obtaining $C(i)$, calibration-based methods can be classified into laboratory and outdoor relative radiometric calibrations, which are performed before launch, as well as into on-orbit/in-flight and ground-based relative radiometric calibrations, which are performed after launch.

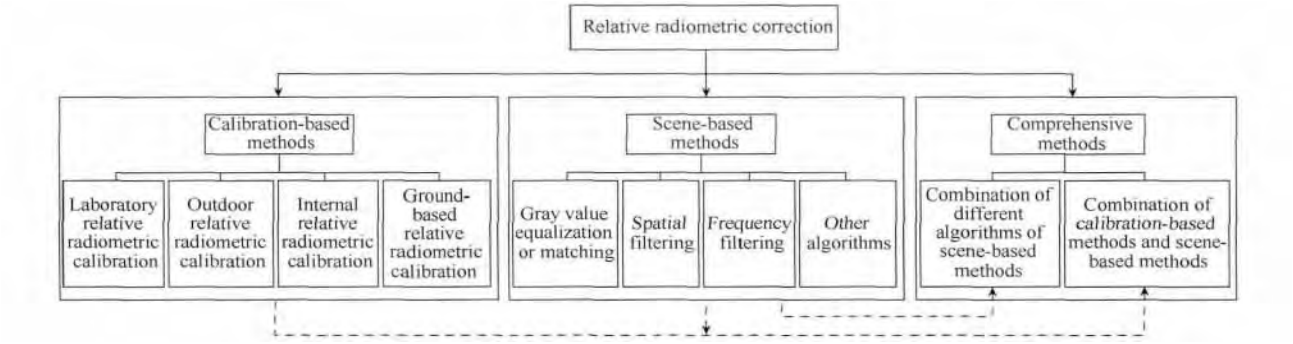

Fig. 1 New classification rule for relative radiometric correction methods

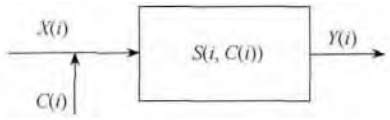

Fig. 2 Schematic of calibration-based methods

(1) Laboratory relative radiometric calibration. This method dates back to 1930 when Ornstein, et al. (1930) proposed a calibration method that uses standard lights, which is the earliest r elative radiometric calibration method. At present, laboratory relative radiometric calibration method collects data in two ways: by "standard lights-diffuser-camera under test" or by "integrating sphere lights-camera under test" (Markham, et al., 1998; Zhang, et al., 2011; Huang, et al., 2013). This method p rovides the highest precision and mature technology. Moreover, it is a necessary step for airborne and space borne sensors before their final assembly. However, the calibration coefficients of a sensor change with launch, aging, and other factors, and thus, other calibration methods are necessary to complement the laboratory calibration.

(2) Outdoor relative radiometric calibration. This method is a new calibration method that uses the sun as the light source (Duan, et al., 2013; Cui, 2009). The principles of this method are as below (1) to use the sensor to observe a u niform target that is illuminated by sunlight and that fills the entire field of view, (2) to evaluate the non-uniformity of the r esponse of CCD detectors, and (3) to obtain the relative radiometric calibration coefficients. This method can eliminate errors caused by differences between the laboratory light source and sunlight with respect to the shapes of spectral lines, color t emperatures, and r adiances, such that parameters that are nearest the working c ondition are o btained. This method can be used for airborne and space borne sensors; however, the calibration result is influenced by the weather condition.

(3) On-orbit/in-flight internal relative radiometric calibration. This method is performed via an internal calibration system c onnected with a remote sensor through two approaches: calibration by using artificial or natural light sources. Artificial light sources typically include standard lights and black bodies. Natural light sources are typically sunlight and moonlight, or the reflection of sunlight. The advantage of internal calibration is providing precise monitoring of sensor performance in realtime. However, the internal calibration system has complex structure, is extremely costly, and huge; and thus, accommodating small satellites and airborne sensors is difficult. Moreover, as the internal calibration system ages, the uncertainty of calibration coefficients increases.

(4) Ground-based relative radiometric calibration. This method, which is also called "homogeneous scenes," calculates calibration coefficients by using homogeneous nature scenes s uch as the sea, ice, or dessert in the image (Chen, 2005; L yon, 2009; Bindschadler & Choi, 2003). This method does not rely on c alibration equipment but is also strict with ground f eatures. However, finding a homo generous scene in the entire field of view is difficult; therefore, ground-based calibration has many limitations for both airborne and space borne sensors. C ertain a lgorithms should be developed to address this disadvantage.

To summarize, calibration-based methods correct images a ccording to the conditions of the remote sensor and exhibit high precision. However, two problems remain in this method. First, calibration is complex and strict with the experimental conditions. Second, the calibration coefficients sometimes do not match the image to be corrected; thus, the calibration coefficients cannot completely reflect the working condition of the sensor. Therefore, scene-based methods have an important role in the relative radiometric correction of remote sensing images, particularly for satellite images.

2.2 Scene-based methods

Scene-based methods are different from calibration-based methods. The former do not require special training data. Instead, these methods obtain relative radiometric correction coefficients from the statistical information of the images themselves. The mathematical model of scene-based methods is illustrated in F ig. 3, where $X(i)$ refers to the original remote sensing image, $M(i)$ is the correction model, and $Y(i)$ is the corrected image. Thus, $Y(i) = X(i)M(i)$.

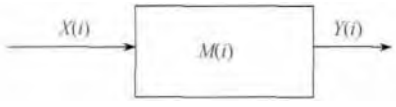

Fig. 3 Schematic of scene-based methods

Based on the principles of correction model $M(i)$, scene-based methods can be classified into gray value equalization or matching, spatial filtering, frequency filtering, MAP-based algo-

rithm, spectral correlation-based algorithm, and uneven illumination correction method, amongothers.

(1) Gray value equalization or matching. This algorithm i ncludes histogram equalization, histogram matching, and moment matching. Histogram equalization was first used in d estriping Landsat images. This algorithm requires an image to have a homogeneous scene or lines that are more than the c olumns (Horn & Woodham, 1979). Histogram matching calculates the histogram of each sensor and matches it with the histogram of the reference sensor to correct an image (Wegener, 1990). Moment matching assumes that each sensor views a s tatistically similar sub-image, and that a linear relationship exists between the gain and the offset of sensors. Based on this linear relationship, the algorithm matches the gain and the offset of each sensor to typical values that are resistant to the effects of outliers (Gadallah, et al., 2000). Frequently, moment matching r esults exhibit better effects than histogram matching results (Liu, et al., 2002).

(2) Spatial filtering. This algorithm is based on the patterns of stripe noises in the spatial domain. Three approaches are used for spatial filtering. The first approach is dead pixel replacement by nearest-neighbor, averaged, or medium values (Ratliff, et al., 2007). The second approach is pixel replacement by convoluting the template (Kenneth, 2002). The third approach is conducting smooth filtering on the column average and standard deviation of raw images to obtain the new column average and standard deviation that can be used to calculate relative radiometric coefficients. Smooth filtering includes average filtering, polynomial fitting, moving window, and averaged adjacent columns (Crippen, 1989; Ballester, et al., 2001; Zhang, et al., 2006). Spatial filtering exhibits rapid computation speed and high efficiency. This algorithm can deal with regular stripe noises effectively. The disadvantage of this algorithm is that it removes some image d etails to smoothen the image.

(3) Frequency filtering. This algorithm considers stripe noises as periodic noises with high frequency, adopts fast Fourier transformor wavelet transform to extract noises, and conducts i nverse transform to obtain the resultant image. According to d ifferent transform algorithms, frequency filtering can be classified into Fourier transform and wavelet transform. Fourier transform typically uses an ideal low-pass filter, a Butterworth low-pass filter, an exponent low-pass filter, a power filter, or afinite impulse response filter (Srinivasan, et al., 1988; Chen, et al., 2003; Simpson, et al., 1998). Wavelet transform detects and r emoves stripe noises by using the direction a land multi-scale properties of wavelet decomposition. In addition to the advantages of Fourier transform, wavelet transform exhibits good localization property in both frequency and spatial domains. The following are typical wavelet transform algorithms: wavelet thresholding (Donoho, 1993; Donoho & Johnstone, 1995), Teager energy o perator (Sankur, et al., 1996), wavelet analysis (Torres & Infante, 2001), and wavelet shrinkage (Yang, et al., 2003). Given that frequency filtering exhibits difficulty in distinguishing ground information from noises, which both have high frequencies, some edges of ground features are lost during filtering.

(4) MAP-based algorithm. Shen and Zhang (2009) developed this algorithm for destriping and inpainting remote sensing images. This algorithm builds a MAP-based recovery model and calculates the gain and offset of detectors by using moment matching. However, this method may degrade the ground resolution of an image because the d erivatives of image pixels are m inimized. Carfantan and Idier (2010) proposed a statistical linear destriping algorithm. This a lgorithm is based on the statistical estimation of each detector gain from an observed image, assuming a linear response. It also assumes that the offset has been removed. Therefore, this algorithm changes the general linear model into a proportional model, and simulates images in the Log domain. The statistical linear destriping algorithm is a new self-calibration destriping technique that does not require special training data. However, this technique is more complex and has not been widely used.

(5) Spectral correlation-based algorithm. Sun, et al. (2008) proposed spectral moment matching based on the property of spectral correlation for a hyper spectral image. This algorithm uses spectral correlation instead of spatial correlation. The high correlation among different bands ensures that the statistical data of bands within a sensor are comparable. Therefore, the band with stripe noises can be corrected. Acito, et al. (2011) developed a subspace-based striping noise reduction model. This algorithm separates signal projection and noise p rojection into two orthogonal subspaces to eliminate noises. Lu, et al. (2013) proposed a graph-regularized low-rank representation for destriping. This a lgorithm uses the low-rank representation technique to exploit the high spectral correlation among observation sub-images in distinct bands, and then incorporates the graph regularizer in the objective function to preserve the intrinsic local structure of original hyperspectral data. The experimental results and the quantitative analysis demonstrate that this algorithm can remove striping noise and achieve cleaner and higher-contrast reconstructed results.

(6) Uneven illumination correction method. To solve the problem of uneven illumination, Li, et al. (2010) proposed a new uneven illumination correction method. In this method, retinex theory and the variational function are used to estimate uneven illumination distribution in an imaging instant. In the variational retinex framework (Land & McCann, 1971; Kimmel, et al., 2003), the projected normal steepest descent optimization method is a pplied to solve the function. Compared with traditional retinex models based on light reflection (Zhang & Shen, 2001) and MASK dodging (Wang & Pan, 2004), this method exhibit obvious advantages in terms of effects and efficiency.

In addition to the aforementioned algorithms, other relative radiometric correction methods are also available, such as the u nidirectional variational model (Bouali & Ladjal, 2011) and the overlapping field-of-view method (Bisceglie, et al., 2009), among others.

Based on the aforementioned analysis, we can determine that unlike calibration-based methods, scene-based methods do not require special training data; thus, the latter can replace the former when the calibration system is invalid or unavailable. However, scene-based methods also have disadvantages. For e xample, the corrected results of these methods rely on the property of images and different correction models. Consequently,

scene-based methods exhibit uncertainties, and the precision of correction coefficients is relatively low. Given that calibration- and scene-based methods both have weaknesses, another group of methods, called comprehensive relative radiometric correction methods, are gradually gaining popularity.

2.3 Comprehensive methods

Comprehensive methods have the characteristics of both calibration- and scene-based methods. These methods are implemented in two ways: (1) by combining different algorithms of scene-based methods and (2) by combining calibration- and scene-based methods. The mathematical model of comprehensive methods is illustrated in Fig. 4, where $X(i)$ refers to the original remote sensing image, $C(i)$ refers to the training data, $S(i)$ is the calibration model, $M(i)$ is the correction model, and $Y(i)$ is the corrected image. Thus, $Y(i) = X(i)S(i, C(i))M(i)$ or $Y(i) = X(i)M_1(i)M_2(i)$.

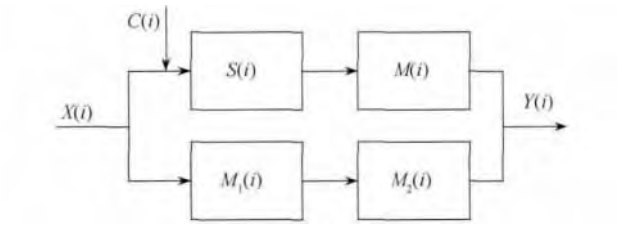

Fig. 4 Schematic of comprehensive methods

(1) Combination of calibration- and scene-based methods. To utilizefully the complementary strengths of calibration- and scene-based methods, Guo, et al. (2005) proposed a relative r adiometric calibration method that uses laboratory calibration and statistical radiometric equalization. This method was applied to correct images acquired by a CCD camera on board the CBERS-02 satellite and successfully eliminated different responses of each CCD chips. Zeng, et al. (2012) proposed a relative radiometric correction method based on laboratory calibration and homogeneous scenes. This method conducts laboratory calibration to obtain correction coefficients, and then uses homogeneous scenes to improve image quality. This method e ffectively eliminated the stripe noises inside a chip and the d ifferent responses of each CCD chip in the Wide Field Imager on board the CBERS-02 satellite. Under the circumstance in which the internal calibration system of a satellite cannot c ompletely eliminate stripe noises, most space borne sensors, such as Landsat TM, Landsat ETM, Landsat ETM +, and MODIS, adopt scene-based methods to improve images (Liu, e t al., 2006).

(2) Combination of different algorithms of scene-based methods. Rakwatin, et al. (2007) proposed a stripe noise reduction method in Terra MODIS and Aqua MODIS data by combining histogram matching with a facet filter. In this method, histogram matching corrects detector-to-detector stripes and mirror side stripes. Then, the iterated weighted least-squares facet filter c orrects noisy stripes. Fuan and Chen (2008) developed an image restoration algorithm by combining stripe detection and spline functions. This image restoration algorithm identifies stripe positions based on edge-detection and line-tracing algorithms. Detected stripes are corrected by replacing the pixels with more r easonable gray values computed from constructed cubic spline functions. Jung, et al. (2010) developed a detection and restoration technique for defective lines in the short-wavelength infrared band of SPOT 4. The detection procedure uses summed and standard deviation data that consist of abnormal peaks originating from defective lines. The defective lines are then restored either by using a moment-matching method or by interpolating. All the aforementioned algorithms exploit the advantages of d ifferent algorithms and correct image through several steps. Therefore, comprehensive methods do not only eliminate stripe noises but also retain the resolution and feature details of the o riginal images.

3 ANALYZING THE APPLICABILITY OF DIFFERENT METHODS

Based on the review of different relative radiometric correction methods both local and abroad, the applicability of these methods and algorithms is comprehensively analyzed in this s ection. Suggestions are also provided on selecting a suitable r elative radiometric correction method.

3.1 Applicability for images with different non-uniform characteristics

Non-uniformity problems include three types: radiometric non-uniformity within the entire image, stripe noises, and defective lines. Therefore, suitable methods should be selected to solve different non-uniformity problems.

In case of stripe noises, given that the spatial distribution and gray values of stripes are typically regular and exhibit certain statistical characteristics, most algorithms of scene-based methods such as gray value equalization or matching, spatial filtering, f requency filtering, MAP-based algorithm, spectral correlation-based algorithm, unidirectional variational model, and overlapping field-of-view method can eliminate stripe noises e fficiently. For example, Han, et al. (2009) adopted an improved moment matching on along-track stripe noises of airborne h yperspectral images. Bouali and Ladjal (2011) used a unidirectional variational model to deal with across-track stripe noises of Aqua MODIS and Terra MODIS images. Chen, et al. (2006) removed oblique stripes of CMODIS images by wavelet transform.

In case of defective lines, considering that the width of d efective lines is frequently 1 pixel to 2 pixels, spatial filtering can solve this problem efficiently. Moreover, experiments show that a MAP-based algorithm, as well as a detection and restoration algorithm for defective lines, will also restore such lines.

In case of non-uniformity within the entire image, experiments show that retinex based on the light reflection model, MASK dodging, and the uneven illumination correction method based on retinex theory can address this problem efficiently. However, these algorithms are not suitable for stripe n oises.

In case of an image that has all three non-uniformity problems, calibration-based methods will function effectively because such methods use the calibration coefficients of a sensor to correct

images and adjust the different responses of each CCD detector individually. For example, He,et al. (2010) adopted laboratory relative radiometric calibration coefficients to correct the high-resolution image of CBERS-02B and to eliminate stripes and defective lines within the image.

3.2 Applicability for images with different geometric characteristics

Generally, different relative radiometric correction methods and algorithms should be selected for images before or after geometric correction. In preprocessing a remote sensing image, relative radiometric correction is typically conducted before geometric correction. As a result, most of the previously discussed methods and algorithms, such as calibration-based methods, gray value equalization or matching, spatial filtering, and the MAP-based algorithm, are designed for images that have not been geometrically corrected. Based on the principle of calibration-based methods, relative radiometric calibration coefficients are only for images in which geometric correction is not yet conducted (Chen, 1997). Chen,et al. (2004) illustrated the different results of moment matching on images before and after geometric correction was conducted individually. Carfantan and I dier (2010) proved that the statistical linear destriping algorithm based on MAP is only suitable for images that have not yet undergone geometric correction.

By contrast, frequency filtering and uneven illumination correction method can be applied on images before and after geometric correction is performed, as proven in a previous research (Li, et al., 2010).

3.3 Applicability for sensor calibration

Given that calibration-based methods have higher precision than other methods; these methods should be used in preference to others if the remote sensor has relative radiometric calibration coefficients or a calibration system. For example, SPOT 1 to SPOT 4 have internal calibration systems; therefore, calibration-based methods reused in image correction. Given that SPOT 5 has no internal calibration system, homogeneous scenes are used in image correction.

In particular, the time of the calibration experiment should be close to the time of remote sensing image acquisition, and the calibration environment should be close to the working environment of the remote sensor. Thus, errors caused by mismatching between sensor calibration and image acquisition can be minimized. If the calibration experiment cannot satisfy the aforementioned requirement, then stripe noises cannot be completely removed by calibration-based methods. In such cases, scene-based methods can be used for further improvement.

3.4 Applicability for images with comprehensive characteristics

Considering that most of relative radiometric correction methods are based on certain theoretical assumptions, different methods should be selected for images with various comprehensive characteristics.

Gray value equalization or matching assumes that each sensor views a statistically similar sub-image. Therefore, this algorithm is suitable for images with large formats and homogeneous scenes. Spatial filtering assumes that the gray values of an image change slowly. Therefore, dead pixel replacement is used, which provides better results for images with regular stripe noises or narrow defective lines. Frequency filtering considers high-frequency signals as stripe noises and allows easy reduction of image details while destriping. Therefore, frequency filtering provides better results for images with simple scenes. Moreover, the statistical linear destriping algorithm is based on the imaging model of a push-broom type sensor; thus, this algorithm is only suitable for push-broom type images. The spectral correlation-based method uses the correction among different bands of a sensor; thus, this method is suitable for destriping hyperspectral images.

3.5 Suggestions on selecting a suitable method

From the aforementioned analysis of the applicability of different relative radiometric correction methods, several contrasting results are drawn (listed in Table 1) based on the following aspects: non-uniformity characteristics, geometric correction, sensor calibration, and the comprehensive characteristics of an image. From Table 1, we can draw the following conclusions. (1) Calibration-based methods can solve all kinds of non-uniformity problems but are only suitable for images without geometric correction. In addition to ground-based relative radiometric calibration, other calibration methods require calibration coefficients or a calibration system. Ground-based relative radiometric calibration requires homogeneous scenes in full view. (2) Scene-based methods employ a number of methods and algorithms that do not require calibration experiments. The six categories of algorithms in Table 1 can solve different non-uniformity problems and demonstrate different applicability for images with various characteristics. (3) Comprehensive relative radiometric correction methods are suitable for different non-uniformity problems. The characteristics and applicability of these methods should be analyzed by case.

In practice, after various factors are considered, the following suggestions on selecting suitable methods are provided. (1) The non-uniformity characteristics of images should be considered first in selecting suitable methods because our main objective is to solve non-uniformity problems. As a result, methods that satisfy the requirements of non-uniformity characteristics should be selected first. (2) Choose suitable methods based on the geometric characteristics of images among the methods selected in the first step. (3) Among the methods selected in the second step, choose suitable methods based on sensor calibration. (4) Make the final decision based on the comprehensive characteristics of images.

3.6 Example of a relative radiometric correction

Based on the suggestions provided in Subsection 3.5, an airborne push-broom type hyperspectral image is corrected by selecting suitable relative radiometric methods.

Table 1 Comparison of applicability among different relative radiometric correction methods and algorithms

Classification	Method/algorithm	Non-uniformity characteristics	Geometric characteristics	Sensor calibration	Comprehensive characteristics	Main references
Calibration-based methods	Laboratory relative radiometric calibration	Non-uniformity, stripe noises, and defective lines	Before geometric correction	Calibration coefficients or a laboratory calibration system are required	No special requirement	Huang, et al. (2013); Markham, et al. (1998)
	Outdoor relative radiometric calibration	Non-uniformity, stripe noises, and defective lines	Before geometric correction	Calibration coefficients or an outdoor calibration system are required	No special requirement	Duan, et al. (2013)
	On-orbit/in-flight internal relative radiometric calibration	Non-uniformity, stripe noises, and defective lines	Before geometric correction	Calibration coefficients ora-n internal calibration system are required	No special requirement	Xiong, et al. (2007); Chang and Xiong (2001)
	Ground-based relative radiometric calibration	Non-uniformity, stripe noises, and defective lines	Before geometric correction	Unnecessary	Suitable for images with homogeneous scenes in full view	Lyon (2009); Bindschadler and Choi (2003)
Scene-based methods	Gray value equalization or matching	Mainly for stripe noises	Before geometric correction	Unnecessary	Suitable for images with large formats and homogeneous scenes	Gadallah, et al. (2000); Horn and Woodham (1979)
	Spatial filtering	Mainly for stripe noises and defective lines	Before geometric correction	Unnecessary	Suitable for images with regular stripe noises or narrow defective lines	Ratliff, et al. (2007); Zhang, et al. (2006)
	Frequency filtering	Mainly for stripe noises and defective lines	No special requirement	Unnecessary	Suitable for images with simple scenes	Chen, et al. (2003); Simpson, et al. (1998)
	MAP-based algorithm	Mainly for stripe noises and defective lines	Before geometric correction	Unnecessary	The MAP-based statistical linear destriping-method is only suitable for images before geometric correction.	Carfantanand and Idier (2010); Shen and Zhang (2009)
	Spectral correlation-based algorithm	Mainly for stripe noises	Before geometric correction	Unnecessary	Suitable for hyperspectral images	Acito, et al. (2011); Sun, et al. (2008)
	Uneven illumination correction method	Mainly for non-uniformity	No special requirement	Unnecessary	Not suitable for images with stripe noises	Land and McCann (1971)
Comprehensive methods	Combination of calibration- and scene-based methods	Non-uniformity, stripe noises, and defective lines	Before geometric correction	Calibration coefficients or a calibration system are required	No special requirement	Guo, et al. (2005)
	Combination of different algorithms of scene-based methods	Non-uniformity, stripe noises, and defective lines	Depends on the algorithms	Unnecessary	Depends on the algorithms	Jung, et al. (2010); Fuan and Chen (2008)

The original image to be corrected is shown in Fig. 5(a). A total of 128 bands exist, and each band has 1024 pixels × 1024 pixels. We can observe several non-uniformity problems in the image, including: radiometric non-uniformity within the entire image, bright and dark stripe noises, and dark lines at the CCD seams. Simultaneously, considering that the hyper spectral imager has relative radiometric calibration coefficients, a calibration-based method is selected to correct the image.

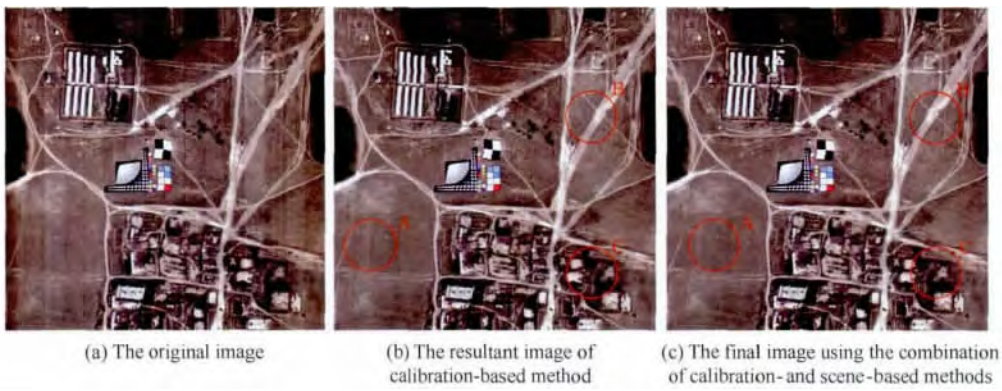

(a) The original image (b) The resultant image of calibration-based method (c) The final image using the combination of calibration- and scene-based methods

Fig. 5 An example of relative radiometric correction using combined calibration- and scene-based methods

For a push-broom type image, the relative radiometric correction model of pixel i in each line is

$$DN_{ci} = \left(DN_{ri} - B_i \right) G_i \quad (1)$$

where DN_{ci} is the corrected digital number (DN) value, DN_{ri} is the original DN value, B_i is the dark current of detector i, and G_i is the normalized gain of detector i. B_i and G_i are acquired from the calibration experiment.

The first correction on the original image is conducted by using Eq. (1), and the result is shown in Fig. 5(b).

From Fig. 5, we can observe that the radiometric non-uniformity within the entire image has been corrected, but slight stripes still appear in the image. These stripes are caused by the differences between the calibration experimental platform on the ground and the airborne platform, such as air pressure, temperature, stability, and so on. As a result, calibration coefficients do not always match with the remote sensing image and are unable to eliminate stripe noises completely.

To solve this problem, a scene-based method is adopted to conduct a second correction. The stripes are detected by a threshold method, and the adjustment coefficients of each column of the image are calculated by a smoothing filter. Through the coefficients, the image is corrected for the second time.

For the resultant image of the calibration-based method, assuming that the mean of column i is $\overline{DN_{ci}}$, the criteria for the stripe noises are

$$\left| \overline{DN_{c(i+1)}} + \overline{DN_{c(i-1)}} - 2\,\overline{DN_{ci}} \right| > \alpha \quad (2)$$

where α is the threshold which is used to detect the abnormal value.

A smoothing filter is used in the location of the stripe noises and a new mean of column $\overline{DN'_{ci}}$ is produced as

$$\overline{DN'_{ci}} = \beta \cdot \overline{DN_{ci}} + \frac{1-\beta}{2}\left[\overline{DN_{c(i-1)}} + \overline{DN_{c(i+1)}} \right] \quad (3)$$

where β stands for the weight of abnormal value in the smoothed one.

Subsequently, the new adjustment coefficients G'_i of pixel i are calculated by:

$$G'_i = \overline{DN'_{ci}} \Big/ \overline{DN_{ci}} \quad (4)$$

Therefore, the final correction model of pixel i in each line is

$$DN'_{ci} = DN_{ci} \cdot G'_i \quad (5)$$

where DN'_{ci} is the DN value after the second correction (both calibration-and scene-based methods are used), DN_{ci} is the DN value after the first correction (only a calibration-based method is used).

After the two steps of correction by using calibration- and scene-based methods are performed, the final result is shown in Fig. 5(c). From this figure, we can observe that the radiometric non-uniformity within the entire image, the bright and dark stripe noises, and the dark lines at the CCD seams have been eliminated. Image quality has obviously improved. The red circles in Fig. 5(a) to Fig. 5(c) show the effects on the three typical ground features before and after correction: wasteland (A), road (B), and residential land (C).

The comparison between the relative radiometric calibration coefficients used in the calibration-based method and the adjustment coefficients used in the scene-based method is presented in Fig. 6. From Fig. 6, we can observe that the two methods have different functions and advantages in image correction. The former is effective in correcting comprehensive non-uniformity problems, where as the latter has advantages in destriping. As a result, combining the two methods will fully apply their complementary strengths.

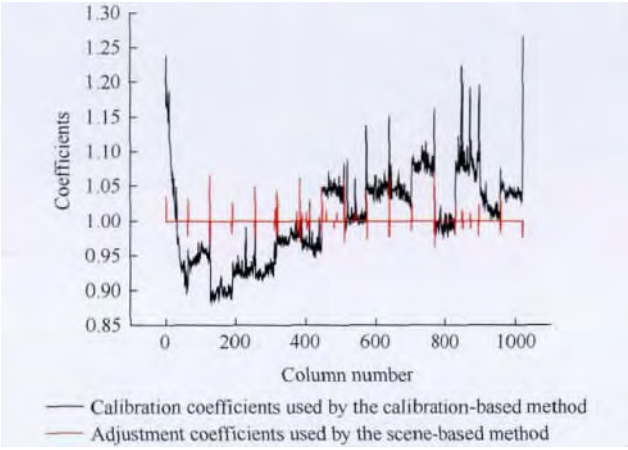

Fig. 6 Comparison between the coefficients used by the calibration- and scene-based methods

4 CONCLUSIONS AND PROSPECTS

Relative radiometric correction of remote sensing images is an important research field in remote sensing data processing that can provide qualified images for the interpretation, information extraction, and quantitative applications of remote sensing. This study reviews the relative radiometric correction methods in the recent 30 years, provides a new classification rule, analyzes the applicability of different methods, and offers suggestions on selecting a suitable method with high precision and efficiency.

The development of quantitative remote sensing prompts the innovation and development of relative radiometric correction. At present, research on relative radiometric correction exhibits the following characteristics. (1) Algorithms are extremely specific. Identifying a method suitable for all kinds of cases among previous relative radiometric correction methods is difficult. The developing requirements for different remote sensors, stripe types, and image types promote an increasing number of specific correction methods and algorithms. (2) The algorithms are comprehensive. Based on the analysis of different algorithms, we can conclude that each algorithm has its own advantages and disadvantages. Therefore, the comprehensive use of different algorithms is an effective means to improve precision. (3) Innovating a mathematical model is crucial. The innovation of relative radiometric correction methods is rooted in the theoretical innovation of digital image processing and the requirements of remote sensing applications. New mathematical models, such as low-dimensional models, local window statistics, and the iterative optimization algorithm, are novel theories that can be applied in relative radiometric correction.

Although research on relative radiometric correction has achieved significant progress and applications, a number of i

mportant problems still need to be addressed.

First, the computer criteria for signal and noises must be e stablished. To date, no algorithm that can eliminate non-u niformity in an image without reducing the details of the image is yet available. Removing noises without influencing effective sig-nals is a problem that should be solved.

Second, the evaluation system of relative radiometric c orrection must be improved. The evaluation method mainly i ncludes qualitative evaluation by visual judgment and quantitative evaluation by image indexes. This method valuates two parts: the preservation of the original image information and the destriping effects. However, no conclusion has been made on determining the optimal method by comprehensively considering these two parts.

Third, the influence of relative radiometric correction on subsequent absolute radiometric corrections requires further stud-ies. Relative radiometric correction is typically conducted before absolute correction and it changes the gray values of an image. As a result, if the old absolute radiometric correction coeffi-cients, i. e. , the conversion coefficients from gray values to radi-ation, are still used in absolute radiometric correction, then the inversed r adiation may be different from the true value. This difference will influence the subsequent quantitative applications of remote sensing data. Researchers should focus on eliminating this influence with respect to quantitative remote sensing.

REFERENCES

Acito N, Diani M and Corsini G. 2011. Subspace-based striping noise r eduction in hyperspectral images. IEEE Transactions on Geoscience and Remote Sensing, 49(4): 1325 - 1342 [DOI: 10. 1109/TGRS. 2010. 2081370]

Ballester C, Bertalmio M, Caselles V, Sapiro G and Verdera J. 2001. Filling-in by joint interpolation of vector fields and gray levels. IEEE Transactions on Image Processing, 10(8): 1200 - 1211 [DOI: 10. 1109/83. 935036]

Bindschadler R and Choi H. 2003. Characterizing and correcting HyPeri-on detectors using ice-sheet images. IEEE Transactions on Geosci-ence and Remote Sensing, 41(6): 1189 - 1193 [DOI: 10. 1109/ TGRS. 2003. 813208]

Bouali M and Ladjal S. 2011. Toward optimal destriping of MODIS data using a unidirectional variational model. IEEE Transactions on Geo-science and Remote Sensing, 49(8): 2924 - 2935 [DOI: 10. 1109/TGRS. 2011. 2119399]

Carfantan H and Idier J. 2010. Statistical linear destriping of satellite-based pushbroom-type images. IEEE Transactions on Geoscience and Remote Sensing, 48(4): 1860 - 1871 [DOI: 10. 1109/TGRS. 2009. 2033587]

Chander G, Helder D L and Boncyk W C. 2002. LANDSAT-4/5 BAND 6 relative radiometry. IEEE Transactions on Geoscience and Remote Sensing, 40(1): 206 - 210 [DOI: 10. 1109/36. 981362]

Chang T J and Xiong X X. 2011. Assessment of MODIS thermal emissive band on-orbit calibration. IEEE Transactions on Geoscience and Re-mote Sensing, 49(6): 2415 - 2425 [DOI: 10. 1109/TGRS. 2010. 2098881]

Chen H S. 1997. Remote Sensing Calibration Systems: An Introduction. Hampton: A. DEEPAK Publishing: 158 - 159

Chen J S, Lin H, Shao Y and Yang L M. 2006. Oblique striping removal in remote sensing imagery based on wavelet transform. International Journal of Remote Sensing, 27(8): 1717 - 1723 [DOI: 10. 1080/ 01431160500185516]

Chen J S, Shao Y, Guo H D, Wang W M and Zhu B Q. 2003. Destrip-ing CMODIS data by power filtering. IEEE Transactions on Geosci-ence and Remote Sensing, 41(9): 2119 - 2124 [DOI: 10. 1109/ TGRS. 2003. 817206]

Chen J S, Shao Y and Zhu B Q. 2004. Destriping CMODIS based on FIR method. Journal of Remote Sensing, 8(3): 227 - 233

Chen Z C. 2005. A Research on the Technology of On-Orbit Calibration and Validation of China DMC Microsatellite. Beijing: Chinese A cademy of Sciences

Corsini G, Diani M and Walzel T. 2000. Striping removal in MOS-B da-ta. IEEE Transactions on Geoscience and Remote Sensing, 38(3): 1439 - 1446 [DOI: 10. 1109/36. 843038]

Crippen R E. 1989. A simple spatial filtering routine for the cosmetic r emoval of scan-line noise from Landsat TM P-tap imagery. Photo-grammetric Engineering and Remote Sensing, 55: 327 - 331

Cui Y. 2009. The Technical Study of Spectrometric Calibration. Xi'an: Chinese Academy of Sciences

di Bisceglie M, Episcopo R, Galdi C and Ullo S L. 2009. Destriping M ODIS data using overlapping field-of-view method. IEEE Transac-tions on Geoscience and Remote Sensing, 47(2): 637 - 651 [DOI: 10. 1109/TGRS. 2008. 2004034]

Dinguirard M and Slater P N. 1999. Calibration of space-multispectral imaging sensors: a review. Remote Sensing of Environment, 68 (3): 194 - 205 [DOI: 10. 1016/S0034 - 4257(98)00111 - 4]

Donoho D L. 1993. Nonlinear wavelet methods for recovery of signals, densities, and spectra from indirect and noisy data. Proceeding of Symposia in Applied Mathematics, 47: 173 - 205

Donoho D L and Johnstone I M. 1995. Adapting to unknown smoothness via wavelet shrinkage. Journal of the American Statistical Associa-tion, 90(432): 1200 - 1224 [DOI: 10. 1080/01621459. 1995. 10476626]

Du P J and Zhao Y D. 2006. Principle of Remote Sensing and Its Appli-cations. Xuzhou: China University of Mining and Technology Press

Duan Y N, Yan L, Yang B, Jing X and Chen W. 2013. Outdoor relative radiometric calibration method using gray scale targets. Science C hina Technological Sciences, 56(7): 1825 - 1834 [DOI: 10. 1007/s11431 - 013 - 5230 - 5]

Fuan T and Chen W W. 2008. Striping noise detection and correction of remote sensing images. IEEE Transactions on Geoscience and R emote Sensing, 46(12): 4122 - 4131 [DOI: 10. 1109/TGRS. 2008. 2000646]

Gadallah F L, Csillag F and Smith E J M. 2000. Destriping multisensor im-agery with moment matching. International Journal of Remote Sensing, 21(12): 2505 - 2511 [DOI: 10. 1080/01431160050030592]

Gao H L, Gu X F, Yu T, Li X Y, Zhi JJ, Xie Y J and Ma X H. 2011. R emoving the stripe noise in HJ-1A HSI images // Proceedings of SPIE, 8203 Remote Sensing of the Environment: The 17th China Conference on Remote Sensing: 820306

Gladkova I, Grossberg M D, Shahriar F, Bonev G and Romanov P. 2012. Quantitative restoration for MODIS band 6 on Aqua. IEEE Transactions on Geoscience and Remote Sensing, 50(6): 2409 - 2416 [DOI: 10. 1109/TGRS. 2011. 2173499]

Guo J N, Yu J, Zeng Y, Xu J Y, Pan Z Q and Hou M H. 2005. The relative radiometric correction of CBERS-01/02 CCD image. Science in China Ser. E(Information Sciences), 35(S1): 11 - 25

Han L, Dong L F, Zhang M and Wu J. 2009. Destriping hyperspectral image based on an improved moment matching method. Acta Optica Sinica, 29(12): 3333 - 3338

He H Y, Wang X Y and Zong Y H. 2010. Relative radiant calibration method and result of TDICCD camera of CBERS-02B satellite. Spacecraft Recovery & Remote Sensing, 31(4): 38 - 44

Henderson B G and Krause K S. 2004. Relative radiometric correction of QuickBird imagery using the side-slither technique on orbit. In: Proceedings of SPIE Earth Observing Systems IX, 5542: 426 - 435 [DOI: 10.1117/12.559910]

Horn B K P and Woodham R J. 1979. Destriping Landsat MSS images by histogram modification. Computer Graphics and Image Processing, 10(1): 69 - 83 [DOI: 10.1016/0146 - 664X(79)90035 - 2]

Huang C P, Zhang L F, Fang J Y and Tong Q X. 2013. A radiometric calibration model for the field imaging spectrometer system. IEEE Transactions on Geoscience and Remote Sensing, 51(4): 2465 - 2475 [DOI: 10.1109/TGRS.2012.2211026]

Jung H S, Won J S, Kang M H and Lee Y W. 2010. Detection and restoration of defective lines in the SPOT 4 SWIR band. IEEE Transactions on Image Processing, 19(8): 2143 - 2156 [DOI: 10.1109/TIP.2010.2046796]

Kenneth R C. 2002. Digital Image Processing. 2nd ed. Beijing: Tsinghua University Press: 447 - 482

Kimmel R, Elad M, Shaked D, Keshet R and Sobel I. 2003. A variational framework for retinex. International Journal of Computer Vision, 52(1): 7 - 23 [DOI: 10.1023/A:1022314423998]

Land E H and McCann J J. 1971. Lightness and Retinex Theory. Journal of the Optical Society of America, 61(1): 1 - 11 [DOI: 10.1364/JOSA.61.000001]

Li H F, Shen H F, Zhang L P and Li P X. 2010. An uneven illumination correction method based on variationalretinex for remote sensing image. Acta Geodaeticaet Cartographica Sinica, 39(6): 585 - 598

Liu J G and Morgan G L K. 2006. FFT selective and adaptive filtering for removal of systematic noise in ETM + imageodesy images. IEEE Transactions on Geoscience and Remote Sensing, 44(12): 3716 - 3724 [DOI: 10.1109/TGRS.2006.881752]

Liu Z J, Wang C Y and Wang C. 2002. Destriping imaging spectrometer data by an improved moment matching method. Journal of Remote Sensing, 6(4): 278 - 284

Lu X Q, Wang Y L and Yuan Y. 2013. Graph-regularized low-rank representation for destriping of hyperspectral images. IEEE Transactions on Geoscience and Remote Sensing, 51(7): 4009 - 4018 [DOI: 10.1109/TGRS.2012.2226730]

Lyon P E. 2009. An automated de-striping algorithm for Ocean Colour Monitor imagery. International Journal of Remote Sensing, 30(6): 1493 - 1502 [DOI: 10.1080/01431160802468263]

Markham B L, Schafer J S, Wood Jr F M, Dabney P W and Barker J L. 1998. Monitoring large-aperture spherical integrating sources with a portable radiometer during satellite instrument calibration. Metrologia, 35(4): 643 - 648 [DOI: 10.1088/0026 - 1394/35/4/72]

Ornstein L S, Vermeulen D and Van Der Held E F M. 1930. Calibration of standard lamps for relative and absolute measurements. Journal of the Optical Society of America, 20(10): 573 - 584 [DOI: 10.1364/JOSA.20.000573]

Pan Z Q, Gu X F, Liu G D and Min X J. 2005. Relative radiometric correction of CBERS-01 CCD data based on detector histogram matching. Geomatics and Information Science of Wuhan University, 30(10): 925 - 927

Pascal V, Lebegue L, Meygret A, Laubies M C, Hourcastagnou J N and Hillairet E. 2003. SPOT 5: first in-flight radiometric image quality results. In Proceedings of SPIE, 4881: 200 - 211 [DOI: 10.1117/12.462633]

Rakwatin P, Takeuchi W and Yasuoka Y. 2007. Stripe noise reduction in MODIS data by combining histogram matching with facet filter. IEEE Transactions on Geoscience and Remote Sensing, 45(6): 1844 - 1856 [DOI: 10.1109/TGRS.2007.895841]

Ratliff B M, Hayat M M and Tyo J S. 2003. Radiometrically accurate scene-based nonuniformity correction for array sensors. Journal of the Optical Society of America, 20(10): 1890 - 1899

Ratliff B M, Tyo J S, Boger J K, Black W T, Bowers D L and Fetrow M P. 2007. Dead pixel replacement in LWIR microgridpolarimeters. Optics Express, 15(12): 7596 - 7609 [DOI: 10.1364/OE.15.007596]

Sankur B, Güler E C and Kahya, Y P. 1996. Multiresolution biological transient extraction applied to respiratory crackles. Computers in Biology and Medicine, 26(1): 25 - 39 [DOI: 10.1016/0010 - 4825(95)00025 - 9]

Shen H F and Zhang L P. 2009. A MAP-based algorithm for destriping and inpainting of remotely sensed images. IEEE Transactions on Geoscience and Remote Sensing, 47(5): 1492 - 1502 [DOI: 10.1109/TGRS.2008.2005780]

Simpson J J, Stitt J R and Leath D M. 1998. Improved finite impulse response filters for enhanced destriping of geostationary satellite data. Optical Engineering, 66(3): 235 - 249

Singh A. 1985. Postlaunch corrections for thematic mapper 5(TM-5) radiometry in the thematic mapper image processing system. Photogrammetric Engineering and Remote Sensing, 51(9): 1385 - 1390

Srinivasan R, Cannon M and White J. 1988. Lands at Data Destriping Using Power Filtering. Optical Engineering, 27: 939 - 943

Sun L X, Neville R, Staenz K and White H P. 2008. Automatic destriping of Hyperion imagery based on spectral moment matching. Canadian Journal of Remote Sensing, 34(S1): 68 - 81

Torres J and Infante S O. 2001. Wavelet analysis for the elimination of striping noise in satellite images. Optical Engineering, 40(7): 1309 - 1314 [DOI: 10.1117/1.1383996]

Wang J N, Gu X F, Ming T and Zhou X. 2013. Classification and gradation rule for remote sensing satellite data products. Journal of Remote Sensing, 17(3): 566 - 577

Wang M and Pan J. 2004. A method of removing the uneven illumination for digital aerial image. Journal of Image and Graphics, 9(6): 744 - 748

Wegener M. 1990. Destriping multiple sensor imagery by improved histogram matching. International Journal of Remote Sensing, 11(5): 859 - 875 [DOI: 10.1080/01431169008955060]

Xiong X X, Sun J Q, Barnes W, Salomonson V, Esposito J, Erives H and Guenther B. 2007. Multiyear on-orbit calibration and performance of Terra MODIS reflective solar bands. IEEE Transactions on Geoscience and Remote Sensing, 45(4): 879 - 889 [DOI: 10.1080/01431169008955060]

Yang Z D, Li J, Menzel W P and Frey R A. 2003. Destriping for MODIS data via wavelet shrinkage. In Proceedings of SPIE, 4895: 187 - 199 [DOI: 10.1117/12.466514]

Zeng Y, Wang W Y and Wang J Q. 2012. A method of relative radiometric calibration based on laboratory calibration and homogeneous scenes. Spacecraft Recovery & Remote Sensing, 33(4): 19 - 24

Zhang B, Zhang H, Chen Z C, Liu X, Luo W F and Zhang L. 2006. A new method of relative radioactive correction based on image statistic. Journal of Remote Sensing, 10(5): 630 - 635

Zhang L F, Huang C P, Wu T X, Zhang F Z and Tong Q X. 2011. Laboratory calibration of a field imaging spectrometer system. Sensors, 11(12): 2408 - 2425 [DOI: 10.3390/s110302408]

Zhang X M and Shen L S. 2001. Image contrast enhancement by wavelet based homomorphic filtering. Acta Electronica Sinica, 29(4): 531 - 533

遥感影像相对辐射校正方法及适用性研究

段依妮[1,2]，张立福[2]，晏磊[1]，吴太夏[2]，刘跃生[3]，童庆禧[1,2]

1. 北京大学 遥感与地理信息系统研究所，北京 100871；
2. 中国科学院 遥感与数字地球研究所，北京 100101；
3. 北京市信息技术研究所，北京 100035

摘　要：遥感影像相对辐射校正是一项基础的数据预处理工作，用于去除影像整体的辐射不均匀性、条带噪声、坏线等辐射问题，经过30多年的发展，已形成几十种不同的相对辐射校正方法和算法。面对种类众多的相对辐射校正方法，它们之间的区别和关联是什么，每种方法的特点是什么，如何选择合适的校正方法，是3个亟需解决的问题。围绕这3个问题，第一，本文以相对辐射校正系数获取的不同方式为原则，将现有的相对辐射校正方法分为3大类：定标法、统计法和综合法，使该分类体系能够反映各类校正方法的区别和关联。第二，在新的分类体系下，给出了定标法、统计法、综合法的数学模型表达，详细介绍了3类方法包含的每种具体的校正方法和算法，比较分析了每种方法的基本思想、原理和优缺点。第三，从影像辐射不均匀特征、影像几何特征、传感器定标、影像综合特征4个方面，对各种校正方法的适用性进行综合分析，给出了科学合理地选择相对辐射校正方法的建议，同时结合具体应用实例进行了实验验证。最后，分析了相对辐射校正研究的发展趋势和存在的问题，有效信息和噪声的计算机判定准则、相对辐射校正效果的评价体系、相对辐射校正对于后续的绝对辐射校正结果的影响是下一步需要深入研究的问题。

关键词：相对辐射校正，定标法，统计法，综合法，适用性分析

中图分类号：P23/TP751　　**文献标志码**：A

引用格式：段依妮，张立福，晏磊，吴太夏，刘跃生，童庆禧. 2014. 遥感影像相对辐射校正方法及适用性研究. 遥感学报，18(3)：597－617

Duan Y N，Zhang L F，Yan L，Wu T X，Liu Y S and Tong Q X. 2014. Relative radiometric correction methods for remote sensing images and their applicability analysis. Journal of R emote Sensing，1 8(3)：597－617　[DOI：10.11834/jrs.20143204]

1　引　言

相对辐射校正又称为去条带校正或均匀化校正，目的是使用相对辐射校正系数作用于原始图像，消除由于传感器或电荷耦合器件CCD(Charge Coupled Device)探元的响应不一致引起的辐射不均匀效应(Dinguirard和Slater，1999)。在遥感卫星数据产品的分级体系中，相对辐射校正是辐射校正的第一级产品，先于绝对辐射定标、大气辐射校正和地形辐射校正，是各类辐射校正的基础(Wang等，2013；杜培军和赵银娣，2006)。

相对辐射校正的种类主要包括影像整体的辐射不均匀、条带噪声、坏线等。很多星载和机载传感器在长期运行过程中，其影像均出现了不同程度、不同种类的辐射不均匀问题，主要是由于光学系统空间响应的不均匀性(如镜头各部分光学透过率的不同)、各个探测器响应的差异、探元的损坏、CCD的暗电流、CCD阵列外电子链路的不一致性等多种原因造成的，需要通过相对辐射校正的手段解决(Corsini等，2000；Chander等，2002；Henderson和Krause，2004)。

相对辐射校正的研究迄今已经历了30余年的发展历程。1985年，Singh(1985)针对Landsat的星上内定标系统，提出一种基于定标法的影像相对辐射校正方法。在此后较长时间内，相对辐射校正系数均由内定标系统给出。基于图像统计的相对辐射校正方法作为一种替代方法用于Landsat的影像校正，但最初只是用于验证定标法的辐射校正精度，直

收稿日期：2013-07-23；修订日期：2013-10-28；优先数字出版日期：2013-11-05
基金项目：国家高技术研究发展计划(863计划)(编号：2012AA121504-2)；环保公益性行业科研专项(编号：2011467071)
第一作者简介：段依妮(1988—　)，女，博士研究生，研究方向为遥感传感器定标、辐射校正。E-mail：yiniduan@126.com
通信作者简介：张立福(1967—　)，男，研究员，博士生导师，研究方向为高光谱遥感理论及应用。E-mail：zhanglf@irsa.ac.cn

到内定标系统元器件的老化使定标法不再可行,才得到充分的发挥(Horn 和 Woodham,1979)。如今,遥感影像的相对辐射校正早已不再局限于上述两种方法,形成了几十种不同的方法和算法(Gao 等,2011;Gladkova 等,2012)。面对种类众多的相对辐射校正方法,它们之间的区别和关联是什么,每种方法的特点是什么,如何选择合适的校正方法,是 3 个亟需回答的问题。

围绕这 3 个问题,本文对现有的相对辐射校正方法进行了系统性的归纳总结;对每种方法的基本思想、原理、优缺点等进行了详细介绍和比较分析;最后,讨论了不同校正方法的适用性,给出了合理选择校正方法的建议。

2 相对辐射校正方法的分类

目前,相对辐射校正方法的分类体系主要有两种:第一,按照校正系数获取的不同方式进行分类,Ratliff 等(2003)、郭建宁等(2005)将相对辐射校正方法分为两大类:定标法和统计法,其中定标法包括基于实验室定标的相对辐射校正、基于内定标的相对辐射校正,统计法包括均匀景统计、直方图均衡、直方图匹配等。第二,按照校正算法实现的不同原理进行分类,Chen 等(2003)将条带去除方法分为直方图匹配法、矩匹配法、数字滤波法、辐射归一化法 4 大类,diBisceglie 等(2009)将条带去除方法分为 3 大类:统计匹配法、空间滤波法、辐射均衡法,Jung 等(2010)将条带去除方法分为两大类:滤波法和调整灰度值分布的方法。

近年来,随着遥感数据种类和数量的快速增长,相对校正方法取得了一系列新的进展,呈现出新的特点,主要包括以下 3 个方面:第一,定标法的适用范围扩大,除内定标之外,学者也尝试采用其他定标方法,如室外相对辐射定标、场地相对辐射定标获取的定标系数进行影像校正,扩展了定标法在传感器运行不同阶段的可用性(Duan 等,2013;Bindschadler 和 Choi,2003)。第二,统计法的种类极大增加,在传统的直方图均衡法、直方图匹配法、矩匹配法的基础上,发展了多种改进方法(刘正军 等,2002;潘志强 等,2005);针对影像条带的问题,引入了数字图像处理中的空域滤波法和频率滤波法,并发展了几十种不同的遥感影像滤波算法(张兵 等,2006;Yang 等,2003);在新型数学模型和交叉学科的影响下,发展了基于最大后验概率 MAP(Maximum A Posteriori)模型的影像条带去除与修复方法、基于变分 Retinex 理论(视网膜大脑皮层理论)的遥感影像不均匀性校正方法等(Shen 和 Zhang,2009;李慧芳 等,2010);针对高光谱影像光谱高度相关的特点,发展了基于子空间的条带噪声去除模型、光谱矩匹配法等(Acito 等,2011;Sun 等,2008)。第三,多种校正方法和算法的综合使用成为趋势,例如综合运用实验室定标和均匀景统计的相对辐射校正方法、综合运用直方图匹配和彩块化滤镜的方法、综合运用条带检测和样条插值修复条带的方法等(曾湧等,2012;Rakwatin 等,2007;Fuan 和 Chen,2008)。

针对相对辐射校正领域出现的上述新方法和新特点,结合现有的分类体系分析可知:Ratliff、郭建宁等提出的分类体系能够在宏观角度清晰地划分不同的校正方法,但现有的多种校正方法和算法综合使用的情况不属于该分类体系。Chen (1997)、diBisceglie 等(2009)以及 Jung 等(2010)提出的分类体系主要是对第一种分类体系中的统计法的子类划分,没有考虑传感器定标在影像校正中的作用。

针对上述问题,本文综合现有分类方法的思路和特点,建立了相对辐射校正方法的新分类体系,如图 1 所示。该体系按照校正系数获取的不同方式,将相对辐射校正方法分为定标法、统计法、综合法 3 大类,并为每类方法下设不同子类,使该分类体系不仅能够反映各类校正方法的区别和关联、涵盖所有的方法,而且具有更好的可扩展性。如图中虚线所示,综合法同时具有定标法和统计法的特征,包括统计法中不同算法的综合,以及定标法与统计法的不同算法的综合。

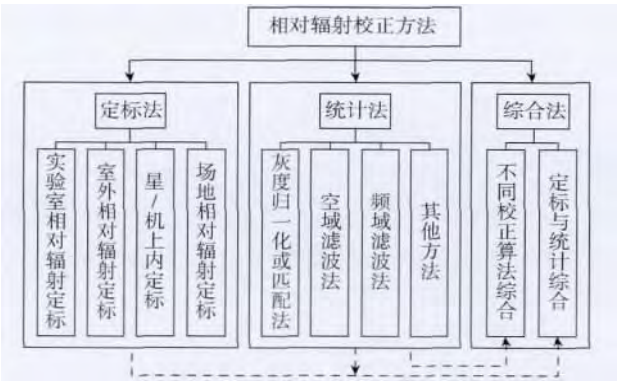

图 1 相对辐射校正方法的新分类体系

2.1 定标法

定标法是指通过传感器定标的方法获取相对辐

射校正系数，从而用于遥感影像的相对辐射校正。由于相对辐射校正系数来源于定标实验，因此定标法需要特殊的训练数据。定标法的数学模型如图 2 所示，其中 $X(i)$ 代表原始遥感影像，i 表示像素编号，$C(i)$ 代表训练数据，$S(i,C(i))$ 代表传感器定标模型，$Y(i)$ 代表校正后遥感影像，则有 $Y(i)=X(i)S(i,C(i))$。

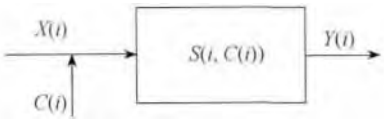

图 2 定标法的原理示意图

按照训练数据 $C(i)$ 获取的不同阶段，定标法主要分为发射前的实验室相对辐射定标、室外相对辐射定标，以及发射后的星/机上内定标和场地相对辐射定标。

(1)实验室相对辐射定标：此方法可追溯到 Ornstein等(1930)提出的基于标准灯的定标方法，是最早出现的传感器相对辐射定标方法。目前，实验室相对辐射定标主要采用“标准灯-漫反射标准板-待测相机”或“积分球-待测相机”方案进行定标数据采集(Markham 等，1998；Zhang 等，2011；Huang 等，2013)。在所有定标法中，实验室定标法精度最高，技术比较成熟，是航空和航天传感器完成总装前的必要环节，但定标系数会随着传感器的发射、老化等因素改变，因此还需其他定标方法作为修正和补充。

(2)室外相对辐射定标：此方法是一种利用太阳作为辐射源的新型定标方法(Duan 等，2013；崔燕，2009)，其基本原理是通过传感器观测太阳照射的充满扫描视场的均匀靶标来评价 CCD 探元响应的不一致性，从而建立精确的传感器相对辐射定标系数。室外相对辐射定标可以克服实验室复色光源与传感器实际工作的太阳光源谱线形状、色温和辐亮度等条件不同导致的误差，能够获得更接近实际工作状态的传感器参数，对航空、航天传感器均适用，但结果会受天气条件的影响。

(3)星/机上内定标：此方法由遥感器内定标系统完成，分为内置定标与向阳定标(Chang 和 Xiong，2001；Xiong 等，2007)。内置定标以标准灯、控温黑体等作为标准光源；向阳定标直接引入太阳、月亮作为光源，或应用较大口径的漫反射板，通过太阳辐射的反射来进行在轨定标。内定标的优点在于能够提供经常性、高精度的定标，但内定标系统结构复杂、成本高、体积大，对于小卫星和航空传感器难以实现。随着内定标系统的老化，采用该方法获取的相对辐射定标系数的不确定性也越来越大。

(4)场地相对辐射定标：此方法又称为“均匀景统计法”，是在传感器飞行过程中，利用地表的均匀自然场景，如大面积的海洋、冰盖或沙漠进行定标(陈正超，2005；Lyon，2009；Bindschadler 和 Choi，2003)。该方法不需要定标设备即可进行，但对地表要求苛刻，难以找到充满全视场的均匀场景，因此在航空、航天应用中均受到限制，需要发展特殊的算法克服场地的不足。

通过上述分析可知，定标法能够从传感器源头入手对影像进行校正，校正精度高，但目前尚存在两个共性问题：一是定标过程复杂、对实验条件要求苛刻；二是定标系数与待校正影像的不匹配性，即传感器定标和影像校正在时间和空间上的分离导致定标结果不能完全反映传感器的真实工作状态。因此，对于很多星载传感器，基于图像统计的相对辐射校正方法起到了重要作用。

2.2 统计法

与定标法不同，统计法不需要特殊的训练数据，通过分析和统计直接从图像中提取校正系数，从而对影像进行校正。统计法的数学模型如图 3 所示，其中 $X(i)$ 代表原始遥感影像，$M(i)$ 代表数学校正模型，$Y(i)$ 代表校正后遥感影像，则有 $Y(i)=X(i)M(i)$。

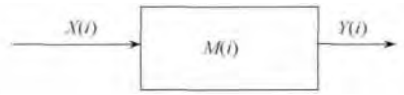

图 3 统计法的原理示意图

按照数学校正模型 $M(i)$ 的实现原理，统计法可分为灰度值归一化或匹配法、空域滤波法、频域滤波法、基于 MAP 模型的方法、光谱相关法、匀光匀色法等。

(1)灰度值归一化或匹配法：此方法主要包括直方图均衡法、直方图匹配法和矩匹配法。直方图均衡法是从 Landsat 发展而来的算法，这种方法要求图像是均匀场景或者图像的行数远远大于探测器的个数(Horn 和 Woodham，1979)。直方图匹配法是计算每个探测器的直方图，并匹配到参考探测器的直方图上，达到对图像相对辐射校正的目的(Wegener，1990)。矩匹配法假设每个传感器对地物探测的辐

射分布是均衡的,传感器之间的增益与漂移值线性相关,根据线性关系,调整各个传感器数据的均值方差到同一个参考值,从而去除条带噪声(Gadallah等,2000)。一般情况下,矩匹配可以获得比直方图匹配更好的效果(刘正军 等,2002)。

(2)空域滤波法:此方法根据条带噪声的空间分布规律性,主要有3种处理方式,第1种是采用最近邻、平均值或中值替代的方法,利用周围的像素值将坏像元填补(Ratliff 等,2007)。第2种是借助模板卷积的方式替换原有像元的灰度值(Kenneth,2002)。第3种是对原始图像的列均值和方差进行平滑处理,获得一组新的列均值和方差,从而求解相对辐射校正系数。平滑处理的方式主要有平均值滤波法、多项式拟合滤波法、移动窗口滤波法、相邻列均衡法等(Crippen,1989; Ballester 等,2001;张兵等,2006)。空域滤波法的运算速度快,效率高,对于遥感影像中规律性的条带噪声具有明显的去除效果。其不足之处是在去除条带的同时也能去除影像的某些细节,使整个影像趋于平滑。

(3)频率滤波法:此方法将条带当作高频周期噪声,采用FFT变换或者小波变换分离出噪声成分,然后利用反变换得到去噪后图像。按照变换方法的不同,可分为傅里叶变换法和小波变换法。傅里叶变换法常用的滤波器有理想低通滤波器、Butterworth低通滤波器、指数低通滤波器、功率滤波器、有限脉冲响应滤波器等(Srinivasan 等,1988;Chen等,2003; Simpson 等,1998)。小波变换利用小波分解的方向及多尺度特性来检测条带和去除条带,在保留了傅里叶变换优点的基础上,能够在频率域与空间域中同时具有良好的局部化特性。几类代表性的算法有:小波阈值法(Donoho,1993;Donoho 和 Johnstone,1995)、"Teager 能量算子"方法(Sankur等,1996)、小波系数去除法(Torres 和 Infante,2001)、小波收缩法(Yang 等,2003)。由于频域滤波法很难将高频的地物信息和高频噪声完全分开,因此在滤波的同时往往会损失掉一些地物边界信息。

(4)基于MAP模型的方法:Shen 和 Zhang(2009)提出的基于MAP模型的影像条带去除与修复方法,通过建立基于MAP的影像复原模型,根据矩匹配的方法确定探元的增益和偏置。该方法尚存在的问题是在对像素的偏导数求最小值的过程中有可能降低地面分辨率。同样基于MAP模型,Carfantan 和 Idier(2010)提出了一种统计线性条带去除法(Statistical Linear Destriping),假设传感器响应函数满足线性,同时偏移量已经被矫正的情况下,将原始的一般线性模型简化成纯线性模型,在Log(对数)域对图像进行建模。该方法属于一种新的自定标去条带技术,不需要特别的训练数据,但算法较复杂,因此尚未得到广泛应用。

(5)光谱相关法:基于高光谱影像的光谱相关性,Sun 等(2008)提出光谱矩匹配法SpcMM(Spectral Moment Matching),采用光谱相关性取代空间相关性,光谱之前的高相关性保证了可以比较同一传感器不同波段的统计量,从而校正具有条带噪声的波段。Acito 等(2011)提出基于子空间的条带噪声去除模型(Subspace-Based Striping Noise Reduction),将信号和噪声分别投影到两个垂直的子空间中,从而将噪声去除,只保留有效信号。Lu 等(2013)提出图像正则化低秩表示的高光谱影像条带去除方法(Graph-Regularized Low-Rank Representation for D estriping),采用低秩表示法寻找不同波段子图像的高光谱相关性,并在目标函数中采用图像正则化矩阵保留高光谱数据原始的局部结构,从而在去除条带的同时,保持图像更清晰和更高的对比度。

(6)匀光匀色法:以影像匀光匀色为目标,李慧芳等(2010)提出的基于变分Retinex理论的遥感影像不均匀性校正方法,是在Retinex理论(Land 和 McCann,1971;Kimmel 等,2003)的基础上,利用变分最优化技术和投影归一化最速下降法求解成像瞬间的照度分布,并以此为基础对遥感影像的灰度不均匀性进行校正。与传统的基于照明反射模型的同态滤波法(张新明和沈兰荪,2001)、Mask 匀光法(王密和潘俊,2004)相比,该方法在校正效果和效率方面均存在明显优势。

此外,遥感影像的相对辐射校正方法还有基于单向变分模型法(Unidirectional Variational Model)(Bouali 和 Ladjal,2011)、重叠瞬时视场角法(Bisceglie 等,2009)等。

通过上述分析可知,与定标法相比,统计法的优势是不需要训练数据,能够在传感器定标系统失效或使用困难时取代定标法。但存在的问题是校正结果依赖图像的选取、数学校正模型的选取,具有一定的人为性,而且获取的定标系数精度普遍较低。由于各类校正方法都有其优势和不足,因此促进了多种校正方法与算法的综合使用,即综合法。

2.3 综合法

综合法同时具有定标法和统计法的特征,通过

两种途径实现：定标与统计综合的方法、不同校正算法综合的方法，数学模型如图 4 所示。其中 $X(i)$ 代表原始遥感影像，$C(i)$ 代表训练数据，$S(i)$ 代表传感器定标模型，$M(i)$ 代表数学校正模型，$Y(i)$ 代表校正后遥感影像，则有 $Y(i)=X(i)S(i,C(i))M(i)$ 或 $Y(i)=X(i)M_1(i)M_2(i)$。

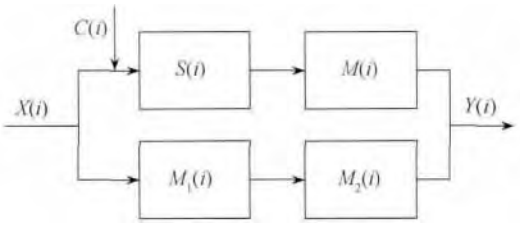

图 4 综合法的原理示意图

（1）定标法与统计法综合：为了实现定标法和统计法的优势互补，郭建宁等（2005）提出一种基于实验室定标和统计辐射度响应归一化的相对辐射校正方法，对 CBERS-02 卫星上搭载的 CCD 相机获取的影像进行校正，成功消除了由于 CCD 拼接导致的片间色差。曾湧等（2012）提出一种基于实验室定标和均匀景统计的相对辐射校正方法，以实验室定标获取的相对辐射定标系数为基础，采用均匀景统计的方法对影像质量进行改善，有效消除了 CBERS-02 卫星宽视场成像仪的影像片内条纹和片间色差。在星上内定标系统不能完全消除影像条带噪声的情况下，Landsat TM、Landsat ETM、Landsat ETM +、MODIS 系列等，均采用统计法辅助进行影像质量的改善（Liu 和 Morgan，2006）。

（2）不同校正算法综合：综合各类校正算法的优点，Rakwatin 等（2007）综合运用直方图匹配和彩块化滤镜（Facet Filter）的方法去除 Terra MODIS 和 Aqua MODIS 影像的严重的条带噪声，其中直方图匹配法用于校正探元之间的条带和镜面条纹，迭代加权最小二乘彩块化滤镜用于消除噪声。Fuan 和 Chen（2008）综合运用条带检测和样条插值的方法用于检测和修复遥感影像的条带噪声，采用边缘检测和线条跟踪算法进行条带位置的确定，采用三次样条函数生成新的像元灰度值 DN（Digital Number），用于替代条带像元。Jung 等人（2010）综合运用坏线检测算法与坏线修复算法去除 SPOT-4 短波近红外波段的条带和坏线，利用影像每列数据的统计特征，判断坏线所在的峰值位置，然后采用矩匹配法或插值的方法消除坏线。

上述方法均充分利用了不同校正算法的优势，分步骤地对影像进行校正，在消除条带的同时，尽可能地保持图像的原始分辨率和纹理细节。

3 各类校正方法的适用性分析

综合国内外学者提出的各种相对辐射校正方法，本节从遥感影像处理的实际需求出发，对每种校正方法的适用性进行分析，并给出了合理选择校正方法的建议。

3.1 辐射不均匀特征对校正方法的要求分析

影像的辐射不均匀特征主要有 3 类：整幅影像的辐射不均匀、条带噪声、坏线。因此，应该针对不同的辐射不均匀问题，选择合适的校正方法。

对于影像主要含有条带噪声的情况，由于条带的空间分布和灰度值通常具有明显的规律和统计特征，因此统计法中的灰度值归一化或匹配法、空域滤波法、频域滤波法、基于 MAP 模型的方法、光谱相关法、基于单向变分模型的方法、重叠瞬时视场角法等可以有效去除条带噪声。例如，韩玲等（2009）采用改进的矩匹配法对机载高光谱影像的沿轨条带进行去除，Bouali 和 Ladjal（2011）采用基于单向变分模型的方法对 Aqua 和 Terra MODIS 影像的穿轨条带进行去除，Chen 等（2006）采用小波变换的方法对神舟 3 号 CMODIS 影像的倾斜条带进行去除。

对于影像含有坏线的情况，由于坏线通常只有 1—2 个像元的宽度，因此空域滤波法可以有效消除坏线。此外，实验结果表明基于 MAP 模型的方法、坏线检测与修复的综合校正法也能够有效消除坏线。

对于影像辐射整体不均匀的情况，实验表明，基于照明反射模型的同态滤波法、Mask 匀光法、基于变分 Retinex 理论的遥感影像不均匀性校正方法能够很好地实现影像匀光匀色功能，但对于条带噪声不能很好地去除。

对于影像同时存在上述 3 类辐射不均匀的情况，由于定标法采用传感器的定标系数进行影像校正，可以对各个探元的响应差异进行调整，因此适用于各类辐射不均匀的校正。例如，何红艳等（2010）采用实验室相对辐射定标系数对 CBERS-02B 卫星的 HR（High Resolution）影像进行了相对辐射校正，有效地消除了条带噪声和坏线。

3.2 影像几何特征对校正方法的要求分析

通常情况下,不同的校正方法对于影像是否经过几何校正有明确的要求。由于遥感影像预处理一般先做相对辐射校正,再做几何校正,因此现有的大多数方法都只适用于几何校正前的影像,如各类定标法、灰度值归一化或匹配法、空域滤波法、基于MAP模型的方法等。从定标法的原理可知,相对辐射定标系数只适用于几何校正前的影像(Chen,1997)。陈劲松等(2004)用实验定量地证明了影像几何校正前后对矩匹配法效果的影响,Carfantan和Idier(2010)通过实验证明了基于MAP的统计线性条带去除法只适用于几何校正前的影像。

与上述方法不同,通常情况下频域滤波法、匀光匀色法对几何校正前后的影像均适用,没有对影像几何校正条件的限制,在已有研究中已经得到了证明(李慧芳 等,2010)。

3.3 传感器定标对校正方法的要求分析

由于定标法的精度较高,若获取影像的传感器具有相对辐射定标系数,或具备定标条件,则可以优先考虑使用定标法进行遥感影像的相对辐射校正。例如,SPOT系列的SPOT 1—SPOT 4卫星上都装有内定标系统,因此主要采用定标法进行影像的相对辐射校正。而SPOT 5没有内定标系统,因此采用地面均匀景统计法对影像进行相对辐射校正(Pascal等,2003)。

需要特别注意的是,定标系数与影像获取的时间应尽量接近,定标环境与传感器运行环境应尽量接近,从而最大限度地减小定标与影像获取不匹配导致的误差。若不满足上述条件,则使用定标法可能无法完全消除影像条带,需使用统计法进一步改善。

3.4 影像综合特征对校正方法的要求分析

由于大多数校正方法的提出都基于一定的理论假设,因此不同的校正方法对影像的综合特征也有不同的要求。

灰度值归一化或匹配的方法通常假设每个传感器所探测的地物具有相同均衡的辐射分布,因此大幅面、地物分布均匀的影像才能满足该统计特征,在使用该方法时才能获得更好的效果。空域滤波法假设影像的灰度是平缓变换的,通常采用周围像元插值的方式修补条带或坏像元,因此对于条带分布有规律、条带或坏线较细的影像能够获得更好的效果。频域滤波法假设高频信号为条带噪声,在去噪的同时也容易去除细节纹理,因此对于地物种类简单的影像能够获得更好的效果。此外,基于MAP的统计线性条带去除法建立在推扫式的探测器成像模型的基础上,因此仅适用于推扫式成像光谱仪的影像校正。光谱相关法建立在各波段光谱高度相关的基础上,因此适用于高光谱影像的条带噪声去除。

3.5 校正方法的选择建议

基于上述相对辐射校正方法在影像辐射特征、影像几何校正、传感器定标条件、影像综合特征4个方面的适用性分析,得出如表1所示的对比分析结果。由表1可知,(1)定标法对各类辐射不均匀的情况均可校正,但只适用于几何校正前的影像,除场地相对辐射定标法外,必须具备传感器定标系数或定标条件,而场地相对辐射定标法要求具备充满全视场的均匀场景。(2)统计法包含的具体校正方法和算法种类繁多,均不需要定标条件即可对影像直接校正。表中列出的六种校正方法对于各类辐射不均匀的问题各有侧重,并且不同的方法对于待校正影像的综合特征具有一定要求。(3)综合法适用于各类辐射不均匀的情况,该方法的特点和适用性需根据选取的算法具体分析。

校正方法的选择需综合考虑多种因素,在实际操作过程中,建议按以下策略进行筛选:(1)由于消除影像的辐射不均匀性是数据处理的最终目标,因此影像辐射特征对校正方法的要求应放在首位考虑,从现有的众多方法中选出几种满足条件的校正方法;(2)根据影像是否经过几何校正,对(1)中选取的方法进行筛选;(3)根据传感器是否具备定标条件,对(2)中选取的校正方法进一步筛选;(4)最后,根据影像的综合特征,并结合校正方法的特点,确定最佳校正方法。

3.6 应用实例

按照3.5节所述的选择策略,对一景航空推扫式高光谱影像进行了相对辐射校正方法的选择和影像校正实例研究。

待校正的原始影像如图5(a)所示,影像共128个波段,每个波段为1024×1024个像元。可以看到影像同时存在多类辐射不均匀问题:整体的辐射不均匀、明暗条带、CCD拼接处的暗线。同时,由于传

感器已具备相对辐射定标系数，因此初步决定采用　　定标法对影像进行校正。

表 1　各类相对辐射校正方法的适用性对比分析结果

类型	方法	影像辐射特征	几何校正	传感器定标	影像综合特征	主要参考文献
定标法	实验室相对辐射定标	辐射不均匀、条带噪声、坏线均可校正	适用于几何校正前的影像	具备定标系数或实验室定标条件	无特殊要求	Huang 等，2013；Markham 等，1998
	室外相对辐射定标	辐射不均匀、条带噪声、坏线均可校正	适用于几何校正前的影像	具备定标系数或室外定标条件	无特殊要求	Duan 等，2013
	星/机上内定标	辐射不均匀、条带噪声、坏线均可校正	适用于几何校正前的影像	具备定标系数或内定标条件	无特殊要求	Xiong 等，2007；Chang 和 Xiong，2001
	场地相对辐射定标	辐射不均匀、条带噪声、坏线均可校正	适用于几何校正前的影像	不需定标条件	具备充满全视场的均匀场景	Lyon，2009 Bindschadler 和 Choi，2003
统计法	灰度值归一化或匹配法	主要用于条带噪声去除	适用于几何校正前的影像	不需定标条件	对于大幅面，地物分布均匀的影像能够获得更好的效果	Gadallah 等，2000；Horn 和 Woodham，1979
	空域滤波法	主要用于条带噪声、坏线去除	适用于几何校正前的影像	不需定标条件	对于条带分布有规律，条带或坏线较细的影像能够获得更好的效果	Ratliff 等，2007；张兵等，2006
	频域滤波法	主要用于条带噪声、坏线去除	无要求	不需定标条件	对于地物种类简单的影像能够获得更好的效果	Chen 等，2003；Simpson 等，1998
	基于 MAP 模型的方法	主要用于条带噪声、坏线去除	适用于几何校正前的影像	不需定标条件	基于 MAP 的统计线性条带去除法仅适用于推扫式成像光谱仪	Carfantan 和 Idier，2010；Shen 和 Zhang，2009
	光谱相关法	主要用于条带噪声去除	适用于几何校正前的影像	不需定标条件	适用于高光谱影像	Acito 等，2011；Sun 等，2008
	匀光匀色法	主要用于辐射不均匀校正	无要求	不需定标条件	对于条带噪声较多的影像效果较差	Land 和 McCann，1971
综合法	定标和统计综合的方法	辐射不均匀、条带噪声、坏线均可校正	适用于几何校正前的影像	具备定标系数或定标条件	无特殊要求	郭建宁 等，2005
	不同校正算法综合的方法	辐射不均匀、条带噪声、坏线均可校正	根据选取的不同算法具体分析	不需定标条件	根据选取的不同算法具体分析	Jung 等，2010；Fuan 和 Chen，2008

图 5　定标法和统计法综合的相对辐射校正实例

对于推扫式影像,任意一行的第 i 个像元的相对辐射校正模型为

$$DN_{ci} = \left(DN_{ri} - B_i\right) G_i \quad (1)$$

式中,DN_{ci} 为定标法校正后的 DN 值,DN_{ri} 为原始 DN 值,B_i 为探元的暗电流值,G_i 为探元的归一化增益,均由传感器定标实验获得。

根据式(1),对原始遥感影像进行第一次校正,校正结果如图 5(b)所示。从图中可以看出,影像整体的辐射不均匀问题已经得到了有效的消除,但仍存在少量细条带。其原因是定标环境与传感器在机上的真实工作状态存在差异,例如气压、温度、平台的稳定性等,造成相对辐射定标系数与影像的不匹配,从而不能完全消除条带噪声。

针对该问题,作者决定采用统计法辅助定标法,进行影像的第 2 次校正:采用阈值法检测条带所在位置,对影像各列的均值进行平滑滤波,计算调整系数,最后采用该套调整系数对整幅影像进行第 2 次校正。

对于定标法校正后的遥感影像,第 i 列的均值用 $\overline{DN_{ci}}$ 表示,条带位置的判定条件为

$$\left|\overline{DN_{c(i+1)}} + \overline{DN_{c(i-1)}} - 2\,\overline{DN_{ci}}\right| > \alpha \quad (2)$$

式中,α 为异常值的判定阈值。

在条带位置进行平滑滤波,形成一个新的列均值 $\overline{DN'_{ci}}$:

$$\overline{DN'_{ci}} = \beta \cdot \overline{DN_{ci}} + \frac{1-\beta}{2}\left[\overline{DN_{c(i-1)}} + \overline{DN_{c(i+1)}}\right] \quad (3)$$

式中,β 为异常值在平滑后的列均值中的权重。

经过上述滤波处理,可得到影像任意一行第 i 个像元的调整系数 G'_i:

$$G'_i = \overline{DN'_{ci}} \Big/ \overline{DN_{ci}} \quad (4)$$

因此,影像任意一行的第 i 个像元的相对辐射校正模型为:

$$DN'_{ci} = DN_{ci} \cdot G'_i \quad (5)$$

式中,DN'_{ci} 为第二次相对辐射校正后的 DN 值(先后采用了定标法和统计法),DN_{ci} 为第一次相对辐射校正后的 DN 值(仅采用了定标法)。

经过定标法和统计法的综合校正,最终结果如图 5(c)所示。由图 5 可以看出,影像整体的辐射不均匀、明暗条带、CCD 拼接处的暗线均得到了有效去除,影像质量有了显著改善。图 5(a)—(c)的红色圆圈分别标出了 3 类典型地物:荒地(A)、道路(B)、居民地(C)的影像校正对比情况。

图 6 给出了定标法采用的相对辐射定标系数和统计法采用的影像调整系数,通过对比可知,定标法和统计法在影像校正中的侧重点和优势不同:定标法能够对影像的整体辐射问题进行调整,统计法在条带噪声处理方法具有优势,因此,将两种方法综合使用能够实现优势互补的效果。

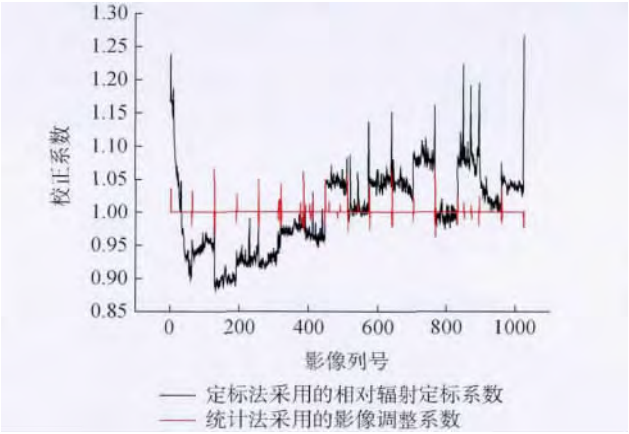

图 6 定标法和统计法采用的影像校正系数对比

4 结 论

遥感影像相对辐射校正是遥感影像数据处理的重要课题之一,为遥感数据的解译、信息提取和各类定量化应用提供符合要求的影像。本文主要对近 30 年来国内外提出的相对辐射校正方法进行了系统的总结和分类,对各类校正方法的适用性进行了详细的比较分析,给出了合理选择校正方法的建议,从而达到既能满足影像校正的精度要求,又能提高效率的最终目的。

遥感信息定量化水平的不断提高对影像质量提出了更高要求,也极大地促进了遥感影像相对辐射校正方法的创新和发展。目前,相对辐射校正方法的发展趋势呈现出以下 3 个特点:(1) 较强的针对性。在现有的各类校正方法中,很难挑选出一种普适性的方法满足各类影像校正的需求。不同传感器、不同的条带表现形式、不同的影像类型等不断出现的新要求,促使更多具有针对性的校正方法和算法的产生;(2) 方法的综合性。通过分析各种相对辐射校正方法及效果可以看出,目前的任何方法都有自身的优缺点,因此,综合利用多种校正方法和算

法实现优势互补，是一个提高校正精度的有效途径；(3) 数学的创新性。相对辐射校正方法的创新根源在于数字图像处理的理论创新以及遥感应用需求的推动。新的数学方法如低维模型(Low-Dimensional Model)、局域窗口统计(Local Window Statistics)以及迭代优化求解的运算方法等，是相对辐射校正可用的创新理论。

目前，尽管相对辐射校正的研究已取得了快速的发展和较好的应用成果，然而仍有一些关键问题亟待解决。

第一，有效信息和噪声的计算机判定准则有待进一步明确。目前还没有一种既不影响影像细节，又能完全消除辐射不均匀的算法。如何在消除影像无效辐射信息的前提下不改变有效辐射信息，仍然是未来需要解决的问题。

第二，影像相对辐射校正效果的评价体系有待完善。目前的校正效果评价方法主要包括目视判断的定性评价和影像质量指标的定量评价。对于影像质量指标，主要考虑原始影像信息的保留程度和条带噪声的去除程度两个方面。然而，如何综合考虑这两个方面的指标来确定最优的校正方法，尚未有明确的结论。

第三，相对辐射校正对于后续的绝对辐射校正结果的影响有待研究。由于相对辐射校正通常先于绝对辐射校正进行，并且改变了整张影像的灰度值，因此在绝对辐射校正的过程中，如果仍然采用原有的绝对辐射定标系数，即灰度值和辐射亮度值之间的转换系数，则反演出的辐亮度影像将与实际情况产生一定差异，这种差异将对后续的定量化应用产生影响。如何消除相对辐射校正对于绝对辐射校正结果的影响，是未来定量遥感需要关注的问题。

参考文献(References)

Acito N, Diani M and Corsini G. 2011. Subspace-based striping noise reduction in hyperspectral images. IEEE Transactions on Geoscience and Remote Sensing, 49(4): 1325 – 1342 [DOI: 10.1109/TGRS.2010.2081370]

Ballester C, Bertalmio M, Caselles V, Sapiro G and Verdera J. 2001. Filling-in by joint interpolation of vector fields and gray levels. IEEE Transactions on Image Processing, 10(8): 1200 – 1211 [DOI: 10.1109/83.935036]

Bindschadler R and Choi H. 2003. Characterizing and correcting HyPerion detectors using ice-sheet images. IEEE Transactions on Geoscience and Remote Sensing, 41(6): 1189 – 1193 [DOI: 10.1109/TGRS.2003.813208]

Bouali M and Ladjal S. 2011. Toward optimal destriping of MODIS data using a unidirectional variational model. IEEE Transactions on Geoscience and Remote Sensing, 49(8): 2924 – 2935 [DOI: 10.1109/TGRS.2011.2119399]

Carfantan H and Idier J. 2010. Statistical linear destriping of satellite-based pushbroom-type images. IEEE Transactions on Geoscience and Remote Sensing, 48(4): 1860 – 1871 [DOI: 10.1109/TGRS.2009.2033587]

Chander G, Helder D L and Boncyk W C. 2002. LANDSAT-4/5 BAND 6 relative radiometry. IEEE Transactions on Geoscience and Remote Sensing, 40(1): 206 – 210 [DOI: 10.1109/36.981362]

Chang T J and Xiong X X. 2011. Assessment of MODIS thermal emissive band on-orbit calibration. IEEE Transactions on Geoscience and Remote Sensing, 49(6): 2415 – 2425 [DOI: 10.1109/TGRS.2010.2098881]

Chen H S. 1997. Remote Sensing Calibration Systems: An Introduction. Hampton: A. DEEPAK Publishing: 158 – 159

Chen J S, Lin H, Shao Y and Yang L M. 2006. Oblique striping removal in remote sensing imagery based on wavelet transform. International Journal of Remote Sensing, 27(8): 1717 – 1723 [DOI: 10.1080/01431160500185516]

Chen J S, Shao Y, Guo H D, Wang W M and Zhu B Q. 2003. Destriping CMODIS data by power filtering. IEEE Transactions on Geoscience and Remote Sensing, 41(9): 2119 – 2124 [DOI: 10.1109/TGRS.2003.817206]

陈劲松，邵芸，朱博勤. 2004. 中分辨率遥感图像条带噪声的去除. 遥感学报，8(3)：227 – 233

陈正超. 2005. 中国 DMC 小卫星在轨测试技术研究. 北京：中国科学院

Corsini G, Diani M and Walzel T. 2000. Striping removal in MOS-B data. IEEE Transactions on Geoscience and Remote Sensing, 38(3): 1439 – 1446 [DOI: 10.1109/36.843038]

Crippen R E. 1989. A simple spatial filtering routine for the cosmetic removal of scan-line noise from Landsat TM P-tap imagery. Photogrammetric Engineering and Remote Sensing, 55: 327 – 331

崔燕. 2009. 光谱成像仪定标技术研究. 西安：中国科学院

di Bisceglie M, Episcopo R, Galdi C and Ullo S L. 2009. Destriping MODIS data using overlapping field-of-view method. IEEE Transactions on Geoscience and Remote Sensing, 47(2): 637 – 651 [DOI: 10.1109/TGRS.2008.2004034]

Dinguirard M and Slater P N. 1999. Calibration of space-multispectral imaging sensors: a review. Remote Sensing of Environment, 68(3): 194 – 205 [DOI: 10.1016/S0034 – 4257(98)00111 – 4]

Donoho D L. 1993. Nonlinear wavelet methods for recovery of signals, densities, and spectra from indirect and noisy data. Proceeding of Symposia in Applied Mathematics, 47: 173 – 205

Donoho D L and Johnstone I M. 1995. Adapting to unknown smoothness via wavelet shrinkage. Journal of the American Statistical Association, 9

0(432): 1200 - 1224 [DOI: 10.1080/01621459.1995.10476626]

杜培军, 赵银娣. 2006. 遥感原理与应用. 徐州: 中国矿业大学出版社

Duan Y N, Yan L, Yang B, Jing X and Chen W. 2013. Outdoor relative radiometric calibration method using gray scale targets. Science China Technological Sciences, 56(7): 1825 - 1834 [DOI: 10.1007/s11431 - 013 - 5230 - 5]

Fuan T and Chen W W. 2008. Striping noise detection and correction of remote sensing images. IEEE Transactions on Geoscience and Remote Sensing, 46(12): 4122 - 4131 [DOI: 10.1109/TGRS.2008.2000646]

Gadallah F L, Csillag F and Smith E J M. 2000. Destriping multisensor imagery with moment matching. International Journal of Remote Sensing, 21(12): 2505 - 2511 [DOI: 10.1080/01431160050030592]

Gao H L, Gu X F, Yu T, Li X Y, Zhi JJ, Xie Y J and Ma X H. 2011. Removing the stripe noise in HJ-1A HSI images // Proceedings of SPIE, 8203 Remote Sensing of the Environment: The 17th China Conference on Remote Sensing: 820306

Gladkova I, Grossberg M D, Shahriar F, Bonev G and Romanov P. 2012. Quantitative restoration for MODIS band 6 on Aqua. IEEE Transactions on Geoscience and Remote Sensing, 50(6): 2409 - 2416 [DOI: 10.1109/TGRS.2011.2173499]

郭建宁, 于晋, 曾湧, 徐建艳, 潘志强, 侯明辉. 2005. CBERS-01/02 卫星 CCD 图像相对辐射校正研究. 中国科学 E 辑(信息科学), 35(S1): 11 - 25

韩玲, 董连凤, 张敏, 吴静. 2009. 基于改进的矩匹配方法高光谱影像条带噪声滤波技术. 光学学报, 29(12): 3333 - 3338

何红艳, 王小勇, 宗云花. 2010. CBERS-02B 卫星 TDICCD 相机的相对辐射定标方法及结果. 航天返回与遥感, 31(4): 38 - 44

Henderson B G and Krause K S. 2004. Relative radiometric correction of QuickBird imagery using the side-slither technique on orbit. In: Proceedings of SPIE Earth Observing Systems IX, 5542: 426 - 435 [DOI: 10.1117/12.559910]

Horn B K P and Woodham R J. 1979. Destriping Landsat MSS images by histogram modification. Computer Graphics and Image Processing, 10(1): 69 - 83 [DOI: 10.1016/0146 - 664X(79)90035 - 2]

Huang C P, Zhang L F, Fang J Y and Tong Q X. 2013. A radiometric calibration model for the field imaging spectrometer system. IEEE Transactions on Geoscience and Remote Sensing, 51(4): 2465 - 2475 [DOI: 10.1109/TGRS.2012.2211026]

Jung H S, Won J S, Kang M H and Lee Y W. 2010. Detection and restoration of defective lines in the SPOT 4 SWIR band. IEEE Transactions on Image Processing, 19(8): 2143 - 2156 [DOI: 10.1109/TIP.2010.2046796]

Kenneth R C. 2002. Digital Image Processing. 2nd ed. Beijing: Tsinghua University Press: 447 - 482

Kimmel R, Elad M, Shaked D, Keshet R and Sobel I. 2003. A variational framework for retinex. International Journal of Computer Vision, 52(1): 7 - 23 [DOI: 10.1023/A:1022314423998]

Land E H and McCann J J. 1971. Lightness and Retinex Theory. Journal of the Optical Society of America, 61(1): 1 - 11 [DOI: 10.1364/JOSA.61.000001]

李慧芳, 沈焕锋, 张良培, 李平湘. 2010. 一种基于变分 Retinex 的遥感影像不均匀性校正方法. 测绘学报, 39(6): 585 - 598

Liu J G and Morgan G L K. 2006. FFT selective and adaptive filtering for removal of systematic noise in ETM + imageodesy images. IEEE Transactions on Geoscience and Remote Sensing, 44(12): 3716 - 3724 [DOI: 10.1109/TGRS.2006.881752]

刘正军, 王长耀, 王成. 2002. 成像光谱仪图像条带噪声去除的改进矩匹配方法. 遥感学报, 6(4): 278 - 284

Lu X Q, Wang Y L and Yuan Y. 2013. Graph-regularized low-rank representation for destriping of hyperspectral images. IEEE Transactions on Geoscience and Remote Sensing, 51(7): 4009 - 4018 [DOI: 10.1109/TGRS.2012.2226730]

Lyon P E. 2009. An automated de-striping algorithm for Ocean Colour Monitor imagery. International Journal of Remote Sensing, 30(6): 1493 - 1502 [DOI: 10.1080/01431160802468263]

Markham B L, Schafer J S, Wood Jr F M, Dabney P W and Barker J L. 1998. Monitoring large-aperture spherical integrating sources with a portable radiometer during satellite instrument calibration. Metrologia, 35(4): 643 - 648 [DOI: 10.1088/0026 - 1394/35/4/72]

Ornstein L S, Vermeulen D and Van Der Held E F M. 1930. Calibration of standard lamps for relative and absolute measurements. Journal of the Optical Society of America, 20(10): 573 - 584 [DOI: 10.1364/JOSA.20.000573]

潘志强, 顾行发, 刘国栋, 闵祥军. 2005. 基于探元直方图匹配的 CBERS-01 星 CCD 数据相对辐射校正方法. 武汉大学学报(信息科学版), 30(10): 925 - 927

Pascal V, Lebegue L, Meygret A, Laubies M C, Hourcastagnou J N and Hillairet E. 2003. SPOT 5: first in-flight radiometric image quality results. In Proceedings of SPIE, 4881: 200 - 211 [DOI: 10.1117/12.462633]

Rakwatin P, Takeuchi W and Yasuoka Y. 2007. Stripe noise reduction in MODIS data by combining histogram matching with facet filter. IEEE Transactions on Geoscience and Remote Sensing, 45(6): 1844 - 1856 [DOI: 10.1109/TGRS.2007.895841]

Ratliff B M, Hayat M M and Tyo J S. 2003. Radiometrically accurate scene-based nonuniformity correction for array sensors. Journal of the Optical Society of America, 20(10): 1890 - 1899

Ratliff B M, Tyo J S, Boger J K, Black W T, Bowers D L and Fetrow M P. 2007. Dead pixel replacement in LWIR microgridpolarimeters. Optics Express, 15(12): 7596 - 7609 [DOI: 10.1364/OE.15.007596]

Sankur B, Güler E C and Kahya, Y P. 1996. Multiresolution biological transient extraction applied to respiratory crackles. Computers in Biology and Medicine, 26(1): 25 - 39 [DOI: 10.1016/0010 - 4825(95)00025 - 9]

Shen H F and Zhang L P. 2009. A MAP-based algorithm for destriping and inpainting of remotely sensed images. IEEE Transactions on Geoscience and Remote Sensing, 47(5): 1492 - 1502 [DOI: 10.1109/TGRS.2008.2005780]

Simpson J J, Stitt J R and Leath D M. 1998. Improved finite impulse r

esponse filters for enhanced destriping of geostationary satellite data. Optical Engineering，66(3)：235 – 249

Singh A. 1985. Postlaunch corrections for thematic mapper 5(TM-5) radiometry in the thematic mapper image processing system. Photogrammetric Engineering and Remote Sensing，51(9)：1385 – 1390

Srinivasan R，Cannon M and White J. 1988. Lands at Data Destriping Using Power Filtering. Optical Engineering，27：939 – 943

Sun L X，Neville R，Staenz K and White H P. 2008. Automatic destriping of Hyperion imagery based on spectral moment matching. Canadian Journal of Remote Sensing，34(S1)：68 – 81

Torres J and Infante S O. 2001. Wavelet analysis for the elimination of striping noise in satellite images. Optical Engineering，40(7)：1309 – 1314 [DOI：10.1117/1.1383996]

Wang J N，Gu X F，Ming T and Zhou X. 2013. Classification and gradation rule for remote sensing satellite data products. Journal of Remote Sensing，17(3)：566 – 577

王密，潘俊. 2004. **一种数字航空影像的匀光方法**. **中国图象图形学报**，9(6)：744 – 748

Wegener M. 1990. Destriping multiple sensor imagery by improved histogram matching. International Journal of Remote Sensing，11(5)：859 – 875 [DOI：10.1080/01431169008955060]

Xiong X X，Sun J Q，Barnes W，Salomonson V，Esposito J，Erives H and Guenther B. 2007. Multiyear on-orbit calibration and performance of Terra MODIS reflective solar bands. IEEE Transactions on Geoscience and Remote Sensing，45(4)：879 – 889 [DOI：10.1080/01431169008955060]

Yang Z D，Li J，Menzel W P and Frey R A. 2003. Destriping for MODIS data via wavelet shrinkage. In Proceedings of SPIE，4895：187 – 199 [DOI：10.1117/12.466514]

曾湧，王文宇，王静巧. 2012. **基于实验室定标和均匀景统计的相对辐射定标方法**. **航天返回与遥感**，33(4)：19 – 24

张兵，张浩，陈正超，刘翔，罗文斐，张靓. 2006. **一种基于图像统计量的相对辐射纠正算法**. **遥感学报**，10(5)：630 – 635

Zhang L F，Huang C P，Wu T X，Zhang F Z and Tong Q X. 2011. Laboratory calibration of a field imaging spectrometer system. Sensors，11(12)：2408 – 2425 [DOI：10.3390/s110302408]

张新明，沈兰荪. 2001. **基于小波的同态滤波器用于图像对比度增强**. **电子学报**，29(4)：531 – 533